

HeteroJIVE: Joint Subspace Estimation for Heterogeneous Multi-View Data

Jingyang Li* Zhongyuan Lyu†

December 3, 2025

Abstract

Many modern datasets consist of multiple related matrices measured on a common set of units, where the goal is to recover the shared low-dimensional subspace. While the Angle-based Joint and Individual Variation Explained (AJIVE) framework provides a solution, it relies on equal-weight aggregation, which can be strictly suboptimal when views exhibit significant statistical heterogeneity (arising from varying SNR and dimensions) and structural heterogeneity (arising from individual components). In this paper, we propose **HeteroJIVE**, a weighted two-stage spectral algorithm tailored to such heterogeneity. Theoretically, we first revisit the “non-diminishing” error barrier with respect to the number of views K identified in recent literature for the equal-weight case. We demonstrate that this barrier is not universal: under generic geometric conditions, the bias term vanishes and our estimator achieves the $O(K^{-1/2})$ rate without the need for iterative refinement. Extending this to the general-weight case, we establish error bounds that explicitly disentangle the two layers of heterogeneity. Based on this, we derive an oracle-optimal weighting scheme implemented via a data-driven procedure. Extensive simulations corroborate our theoretical findings, and an application to TCGA-BRCA multi-omics data validates the superiority of **HeteroJIVE** in practice.

Author names are sorted alphabetically.

*University of Michigan, Ann Arbor. Email: jjyyli@umich.edu.

†The University of Sydney. Email: zhongyuan.lyu@sydney.edu.au.

1 Introduction

In modern applications, data are often recorded as collections of matrices on a common set of units. Examples include computational biology, where the same tissue samples are profiled by multiple assays in TCGA (Network, 2012; Lock et al., 2013; Zhang and Gaynanova, 2022; Sergazinov et al., 2024), chemometrics, where the same chemicals are characterized by multiple instruments (Smilde et al., 2003; Löfstedt et al., 2013), and autonomous driving, where synchronized sensors (cameras, LiDAR, radar) are recorded for the same time-stamped scenes (Geiger et al., 2013; Caesar et al., 2020). In all these examples, the data can be represented by K matrices $\{\mathbf{A}_k\}_{k=1}^K$, and each \mathbf{A}_k is of dimension n by d_k , where n is the number of units and d_k is the view-specific dimension. It is often interesting to identify the joint latent structure among \mathbf{A}_k 's while allowing view-specific structures to persist. For instance, on TCGA multi-omics, the joint low-dimensional space captures subtype structure while individual parts retain assay-specific effects (gene expression, miRNA, genotype, protein/RPPA), and ignoring the individual structure can lead to severe information loss (Lock et al., 2013; Gaynanova and Li, 2019).

The Joint and Individual Variation Explained (JIVE) framework (Lock et al., 2013) formalizes this by assuming data matrices $\{\mathbf{A}_k\}_{k=1}^K$ admit the following decomposition:

$$\mathbf{A}_k = \mathbf{U}\mathbf{V}_k^\top + \mathbf{U}_k\mathbf{W}_k^\top + \mathbf{E}_k \in \mathbb{R}^{n \times d_k}, \quad k \in [K]. \quad (1)$$

Here $\mathbf{U} \in \mathbb{O}_{n,r}$ and $\mathbf{U}_k \in \mathbb{O}_{n,r_k}$ are the *joint* and *individual* subspaces, respectively, where $\mathbb{O}_{p,q}$ denotes the space of orthonormal matrices of dimension p by q , $\mathbf{V}_k \in \mathbb{R}^{d_k \times r}$ and $\mathbf{W}_k \in \mathbb{R}^{d_k \times r_k}$ are the loading matrices, and \mathbf{E}_k is the random noise. It is commonly assumed that $r + r_k \ll n \wedge d_k$ for all $k \in [K]$, so that one can leverage the spectral method to exploit the low-rankness of $\mathbf{U}\mathbf{V}_k^\top + \mathbf{U}_k\mathbf{W}_k^\top$. Among the most popular algorithms for this task, Angle-based JIVE (AJIVE) (Feng et al., 2018) first estimates the joint and individual subspaces $\begin{bmatrix} \mathbf{U} & \mathbf{U}_k \end{bmatrix}$ by performing SVD on each \mathbf{A}_k individually, denoted by $\tilde{\mathbf{U}}_k$, then aggregates the results to estimate the shared subspace \mathbf{U} via a second SVD, i.e.,

$$\hat{\mathbf{U}} = \text{Eigen}_r \left(\sum_{k=1}^K \tilde{\mathbf{U}}_k \tilde{\mathbf{U}}_k^\top \right),$$

where $\text{Eigen}_r(\mathbf{A})$ denotes the leading- r eigenvectors of matrix \mathbf{A} . Though equipped with different names, this two-stage spectral algorithm has been widely used in many integrative

analyses (Fan et al., 2019; Arroyo et al., 2021; Li et al., 2024; Tang et al., 2025) due to its computational efficiency.

The standard AJIVE algorithm implicitly assumes that all views contribute equally to the estimation of the joint space. Nonetheless, a pervasive feature of multi-view data in practice is heterogeneity across views, i.e., the SNR and view-specific dimensions $\{d_k\}_{k=1}^K$ of \mathbf{A}_k 's may vary substantially from one view to another. We term this *statistical heterogeneity*. In such cases, equal-weight aggregation in the second step of AJIVE can be suboptimal, as it treats all views as equally informative. We illustrate this limitation with the following toy example.

Example 1. Consider $K = 2$, $\mathbf{A}_1 = \mathbf{U}\mathbf{W}^\top + 2\mathbf{U}_1\mathbf{V}^\top + \mathbf{E}_1$ and $\mathbf{A}_2 = 100(\mathbf{U}\mathbf{W}^\top + 2\mathbf{U}_2\mathbf{V}^\top) + \mathbf{E}_2$, where $\mathbf{E}_1, \mathbf{E}_2 \stackrel{\text{i.i.d.}}{\sim} N(0, 0.1^2)$. In this case, the performance of $\hat{\mathbf{U}} := \text{Eigen}_r(\tilde{\mathbf{U}}_0\tilde{\mathbf{U}}_0^\top + \tilde{\mathbf{U}}_1\tilde{\mathbf{U}}_1^\top)$ is largely deteriorated by the low-SNR of \mathbf{A}_1 . At the same time, direct SVD solely on \mathbf{A}_2 failed to identify \mathbf{U} due to the factor 2 in front of the individual component $\mathbf{U}_2\mathbf{V}^\top$.

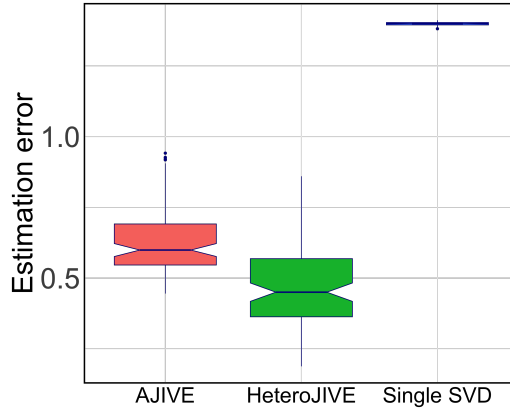


Figure 1: Estimation error of $\|\hat{\mathbf{U}}\hat{\mathbf{U}}^\top - \mathbf{U}\mathbf{U}^\top\|$ across methods for Example 1 averaged over 100 replicates. The average weights for HeteroJIVE are given by (0.011, 0.989).

Beyond statistical heterogeneity, the JIVE model introduces a more fundamental challenge. Unlike standard multi-view low-rank models which assume data consist solely of a low-rank component and noise (i.e., $\mathbf{A}_k = \mathbf{U}\mathbf{V}^\top + \mathbf{E}_k$) (Hong et al., 2023; Ma and Ma, 2024; Baharav et al., 2025), the JIVE framework explicitly incorporates view-specific individual

variations $\{\mathbf{U}_k \mathbf{W}_k^\top\}_{k=1}^K$. We term the interaction between these individual subspaces and the joint subspaces as *structural heterogeneity*.

To address these challenges, we propose **HeteroJIVE**, a weighted AJIVE-type estimator tailored to heterogeneity. In the high-level, **HeteroJIVE** retains the two-stage structure of AJIVE but replaces the equal-weight aggregation with a weighted average of the first-stage estimates. By down-weighting views with lower SNR or higher interference, we prevent noisy views from contaminating the joint signal. Consequently, the optimal weights must account for both layers of heterogeneity. While no general closed form exists for the optimal weights, we explicitly disentangle statistical and structural heterogeneity via a delicate analysis, which motivates a computationally efficient, data-driven weighting scheme with strong empirical performance. For illustration, we consider the setup in Example 1, and Figure 1 demonstrates that **HeteroJIVE** significantly outperforms both AJIVE and single SVD (on \mathbf{A}_2). Notably, even with a negligible weight (0.011) assigned to the noisy view \mathbf{A}_1 , integrating both views yields superior identification compared to using \mathbf{A}_2 alone.

While **HeteroJIVE** addresses heterogeneity empirically, establishing its theoretical guarantees reveals a deeper challenge intrinsic to the JIVE framework. Even for AJIVE, its statistical guarantee has only recently been clarified, especially under the large- K regime. In particular, Yang and Ma (2025) establishes fundamental limits of AJIVE, identifying a “non-diminishing” barrier in the estimation error: in low-SNR regimes, a second-order bias term does not vanish as even as K increases.

In this paper, by explicitly analyzing the orientation between joint and individual loadings, we demonstrate that the bias term naturally diminishes under mild geometric conditions. Our analysis provides a unified upper bound that not only matches the $O(K^{-1/2})$ rate in favorable regimes but also yields a strictly tighter error bound than existing results in general settings.

1.1 Main contributions

Our contributions are multi-fold, spanning algorithm, theory, and practice.

First, in terms of algorithm, we propose **HeteroJIVE**, a weighted spectral method tailored for joint subspace recovery of multi-view data under two-layer heterogeneity. Unlike standard approaches that treat views equally, our method incorporates a weighting mech-

Table 1: Comparison of theoretical guarantees of our framework under the equal-weight case (i.e., AJIVE) with the results of [Yang and Ma \(2025\)](#) and [Tang et al. \(2025\)](#). For deterministic loadings, explicit forms of the error rates are deferred to Section 3. For random loadings, our results in the table assume that the individual subspaces $\{\mathbf{U}_k\}_{k=1}^K$ are also random, to facilitate comparison with [Tang et al. \(2025\)](#). Here, ε denotes the subspace estimation error of the initial SVD on a single view, and θ characterizes the alignment of individual subspaces $\{\mathbf{U}_k\}_{k=1}^K$.

		Deterministic		Random	
		Yang and Ma (2025)	This paper	Tang et al. (2025)	
Model		JIVE with equal σ_k 's	General JIVE		JIVE with $\mathbf{W}_k = \mathbf{W}$
Algorithm		Two-stage spectral	Two-stage spectral		Two-stage spectral followed by iterative refinement
Error rate	w.r.t. K	Non-vanishing bound as $K \rightarrow \infty$	Sharper bound, vanishing in K under certain condition	Optimal rate decay at $\tilde{O}(\varepsilon K^{-1/2})$	Initialization error decay at $O(\varepsilon^2)$; Refinement error decay at $\tilde{O}(K^{-1/2})$
	w.r.t. ε	First-order suboptimal when $K\theta \lesssim 1$	First-order optimal		
Condition on K		None	None	$K \gtrsim \log n$	$K \gtrsim \varepsilon^{-4} \log n$

anism into the spectral aggregation step.

Second, on the theoretical front, we establish a general framework that refines previous results within comparable settings. Our analysis yields several key insights. We revisit the “non-diminishing” error barrier for AJIVE, a limitation previously identified by [Yang and Ma \(2025\)](#), and we demonstrate that this barrier is not universal but rather an artifact of specific worst-case geometric configurations. Our analysis reveals that the non-vanishing bias effectively cancels out when individual loadings are nearly orthogonal or randomly oriented. Consequently, we prove that the joint subspace estimation error decays at the optimal $O(K^{-1/2})$ rate with respect to the number of views. This result suggests that simple, non-iterative spectral methods are minimax-optimal in a much broader regime than previously understood, achieving rates comparable to iterative refinement techniques like those in [Tang et al. \(2025\)](#) but under weaker requirements on K . We summarize the above contributions in Table 1. Furthermore, we extend our theory to the general heterogeneous

setting with non-asymptotic error bounds explicitly disentangling statistical heterogeneity from structural heterogeneity. Building on this, we develop an oracle-optimal weighting algorithm to select optimal weights. Notably, in the specific regime where individual components are absent, our derived weights and error rates strictly align with the recent optimality results for SVD-Stack established by Baharav et al. (2025).

Finally, bridging theory and practice, we provide a data-driven implementation for the oracle-optimal weighting algorithm, which is computationally simple and empirically effective. Extensive numerical simulations corroborate our theoretical findings, and an application to TCGA-BRCA multi-omics data validates the superiority of HeteroJIVE, demonstrating the advantage of explicitly accounting for heterogeneity in practice.

1.2 Related Work

Our work is closely related to recent developments in AJIVE, heterogeneous PCA, and distributed/federated PCA. Regarding statistical guarantees for JIVE, Ma and Ma (2024) analyze Stack-SVD for the special case of $K = 2$. However, their result requires prior knowledge of the column indices of \mathbf{U} within the singular vectors of the stacked signal matrix. In a broader setting, Baharav et al. (2025) systematically compare Stack-SVD, SVD-Stack, and their weighted variants, though their asymptotic analysis assumes the absence of individual components (i.e., $\mathbf{U}_k \mathbf{W}_k^\top = 0$). The most relevant work to ours is Yang and Ma (2025), which analyzes AJIVE under a homogeneous setting. They show that AJIVE attains an $O(K^{-1/2})$ rate in a high-SNR regime, but the error bound contains a non-vanishing term as K increases when the SNR is low. In parallel, Tang et al. (2025) study a multi-view spiked covariance model (where $d_k = d$ and $\mathbf{W}_k = \mathbf{W}$) and propose the MOP-UP algorithm, which combines an AJIVE-type initialization with alternating projections. In contrast, our analysis of the matrix JIVE model suggests that such iterative refinement is likely redundant for achieving the optimal rate.

More broadly, our framework lies in the literature on PCA under heterogeneity. One line of work mainly models statistical heterogeneity (Oba et al., 2007; Zhang et al., 2022; Arroyo et al., 2021; Hong et al., 2023; Yan et al., 2024), while another focuses on heterogeneous individual components (Lock et al., 2013; Zhou et al., 2015; Shi and Al Kontar, 2024). Most of these methods encode noise heterogeneity at the modeling level and then demonstrate a

certain robustness to heterogeneity, either theoretically or empirically, but do not explicitly adjust the estimation procedure to exploit it. This is likely to be suboptimal, especially when a few high-SNR views carry most of the information. Two exceptions are [Oba et al. \(2007\)](#); [Hong et al. \(2023\)](#), both of which propose reweighting an empirical loss to account for heteroskedastic noise and derive optimal weights in their settings. However, they only handle the heterogeneity in noise, and how to extend their weighting schemes to two-layer heterogeneity remains unclear.

Finally, we note that our proposed HeteroJIVE can be computed in a distributed fashion across local machines: each site computes its own local low-rank approximation and sends only a low-dimensional summary to a central server, where the weighted aggregation step is performed. This architecture is closely aligned with the literature on distributed PCA ([Liang et al., 2014](#); [Fan et al., 2019](#); [Zheng and Tang, 2022](#)) and federated PCA ([Grammenos et al., 2020](#); [Li et al., 2024](#)), and makes HeteroJIVE suitable for large-scale or privacy-constrained multi-view data where raw samples cannot be pooled.

1.3 Notation

For any positive integer n , we denote the set of integers $\{1, \dots, n\}$ by $[n]$. We use bold-face capital letters (e.g. \mathbf{A}, \mathbf{E}) to denote matrices, bold-face lower-case letters (e.g. \mathbf{x}, \mathbf{y}) for vectors. We denote by $\|\cdot\|_F$ the Frobenius norm and $\|\cdot\|$ the operator norm of matrices. We denote by $\lambda_i(\mathbf{A})$ the i -th largest singular value of \mathbf{A} . When $n = r$, we simply write \mathbb{O}_n for the orthogonal group. For two real numbers a, b , we use $a \wedge b = \min(a, b)$ and $a \vee b = \max(a, b)$. Finally, let c, C, C_1, \dots denote generic positive constants whose values may change from line to line. We write $a \lesssim b$, $b \gtrsim a$ or $a = O(b)$ if $a \leq Cb$ for a universal constant $C > 0$ and $a \asymp b$ if $a \lesssim b$ and $b \lesssim a$ hold simultaneously. Additionally, we use $\tilde{O}(\cdot)$ to denote order notation ignoring logarithmic factors.

2 Preliminaries for JIVE

2.1 The JIVE Decomposition

We consider the multi-view setting where data are collected as a collection of K matrices $\{\mathbf{A}_k\}_{k=1}^K$ on a common set of n units. We assume the data admit the following JIVE

decomposition:

$$\mathbf{A}_k = \mathbf{U}\mathbf{V}_k^\top + \mathbf{U}_k\mathbf{W}_k^\top + \mathbf{E}_k \in \mathbb{R}^{n \times d_k}, \quad k \in [K]. \quad (2)$$

Here $\mathbf{U} \in \mathbb{O}_{n,r}$ and $\mathbf{U}_k \in \mathbb{O}_{n,r_k}$ are the joint and individual subspaces with $\mathbf{U}^\top \mathbf{U}_k = 0$ for all $k \in [K]$ following [Lock et al. \(2013\)](#); [Yang and Ma \(2025\)](#). This orthogonality constraint entails no loss of generality, as any decomposition in (2) can be equivalently reparameterized to enforce orthogonality. The matrices $\mathbf{V}_k \in \mathbb{R}^{d_k \times r}$ and $\mathbf{W}_k \in \mathbb{R}^{d_k \times r_k}$ denote the view-specific loadings for the joint and individual components, respectively, which can be either deterministic or random in what follows. Finally, \mathbf{E}_k represents the additive noise containing i.i.d. $N(0, \sigma_k^2)$ entries, and allows for heteroskedastic noise levels σ_k 's across views.

2.2 Angle-Based Estimation

To estimate the joint subspace \mathbf{U} , we adopt the angle-based JIVE (AJIVE) framework proposed by [Feng et al. \(2018\)](#). The procedure operates in two stages:

1. **(Signal Extraction)** For each view k , perform an SVD on \mathbf{A}_k and retain the top $r + r_k$ left singular vectors, denoted as $\tilde{\mathbf{U}}_k$.
2. **(Subspace Aggregation)** Estimate the joint subspace \mathbf{U} by aggregating the projection matrices of these local subspaces as $\sum_{k=1}^K \tilde{\mathbf{U}}_k \tilde{\mathbf{U}}_k^\top$.

While the original AJIVE algorithm ([Feng et al., 2018](#)) and recent theoretical analyses ([Yang and Ma, 2025](#)) utilize an unweighted aggregation, we propose HeteroJIVE, a more general weighted spectral estimation scheme. Specifically, we estimate $\hat{\mathbf{U}}$ as the top r left eigenvectors of the weighted sum of projection matrices $\sum_{k=1}^K w_k \tilde{\mathbf{U}}_k \tilde{\mathbf{U}}_k^\top$ where $\{w_k\}_{k=1}^K$ are non-negative weights satisfying $\sum_{k=1}^K w_k = 1$. This formulation, summarized in Algorithm 1, encompasses the standard AJIVE (where $w_k = 1/K$) as a special case, while allowing for the down-weighting less informative views.

A seemingly natural alternative is to stack the data and directly compute the top r eigenvectors of the pooled covariance $\sum_{k=1}^K w_k \mathbf{A}_k \mathbf{A}_k^\top$. However, this approach assumes that individual components are uniformly weak compared to the joint component. When this assumption is violated, directions dominated by strong individual variation can be

mistakenly identified as joint (see Example 1 or the discussion in Yang and Ma (2025)). AJIVE circumvents this by decoupling subspace orientation from signal magnitude. By stripping singular values to normalize subspace scales, the algorithm aggregates via principal angles rather than variances. This ensures the joint subspace estimation is robust to heterogeneous signal strengths (see Algorithm 1).

Algorithm 1 HeteroJIVE

Input: $\{\mathbf{A}_k\}_{k=1}^K$, r , $\{r_k\}_{k=1}^K$, $\{w_k\}_{k=1}^K$

for $k = 1, \dots, K$ **do**

Let $\tilde{\mathbf{U}}_k$ be the top $r + r_k$ left singular vectors of \mathbf{A}_k .

end for

Let $\hat{\mathbf{U}}$ be top r left eigenvectors of $\sum_{k=1}^K w_k \tilde{\mathbf{U}}_k \tilde{\mathbf{U}}_k^\top$.

Output: $\hat{\mathbf{U}}$

3 Theoretical Guarantees

A primary challenge in deriving a sharp estimation error bound for $\hat{\mathbf{U}}$ stems from the algorithm’s reliance on two nested SVD steps. Consequently, the final estimator $\hat{\mathbf{U}}$ is a highly nonlinear functional of the data, constructed from $\tilde{\mathbf{U}}_k$ which are themselves nonlinear. To rigorously control this compounded error, we apply the explicit formula for spectral projector developed in Xia (2021).

We structure our analysis into two parts: the equal-weight case (Section 3.2), which serves as a baseline comparison to existing literature, and the general-weight case (Section 3.3), which addresses heterogeneity. For each setting, we analyze two scenarios for loading matrices $\{\mathbf{V}_k, \mathbf{W}_k\}_{k=1}^K$, either deterministic or random.

3.1 Key Quantities and Assumptions

For each $k \in [K]$, we denote $\bar{r}_k := r + r_k$ and the signal strength $\lambda_{k,\min} := \lambda_{\bar{r}_k}(\mathbf{U}\mathbf{V}_k^\top + \mathbf{U}_k\mathbf{W}_k^\top)$ is the \bar{r}_k -th largest singular value. In addition, we define the condition number and the signal-to-noise ratio (SNR) for k -th view as $\kappa_k := \lambda_{k,\min}^{-1} \|\mathbf{U}\mathbf{V}_k^\top + \mathbf{U}_k\mathbf{W}_k^\top\|$ and $\text{SNR}_k := \lambda_{k,\min}/\sigma_k$, respectively.

Recall from single-view PCA that the unilateral subspace $\bar{\mathbf{U}}_k = [\mathbf{U} \ \mathbf{U}_k]$ has estimation error in operator norm of order (Cai and Zhang, 2018):

$$\left\| \tilde{\mathbf{U}}_k \tilde{\mathbf{U}}_k^\top - \bar{\mathbf{U}}_k \bar{\mathbf{U}}_k^\top \right\| \lesssim \text{SNR}_k^{-1} \sqrt{n} + \text{SNR}_k^{-2} \sqrt{nd_k} =: \varepsilon_k. \quad (3)$$

For HeteroJIVE, the shared-subspace error will appear as a low-degree polynomial in $\{\varepsilon_k\}_{k=1}^K$, capturing cross-view accumulation. Within each view, leakage from individual to joint is governed by the angle between column spaces spanned by \mathbf{V}_k and \mathbf{W}_k , measured by

$$\delta_k := \left\| (\mathbf{V}_k^\top \mathbf{V}_k)^{-1/2} \mathbf{V}_k^\top \mathbf{W}_k (\mathbf{W}_k^\top \mathbf{W}_k)^{-1/2} \right\|. \quad (4)$$

Notice $\delta_k < 1$ (or equivalently, $\lambda_{k,\min} > 0$) is a sufficient condition to ensure $\text{span}(\mathbf{U}) \subset \bigcap_{k=1}^K \text{span}(\mathbf{U} \mathbf{V}_k^\top + \mathbf{U}_k \mathbf{W}_k^\top)$ for identifiability, which is called the faithfulness assumption in Yang and Ma (2025). We will see how δ_k influences the final estimation.

When \mathbf{V}_k and \mathbf{W}_k are treated as random, the observed features can be viewed as realizations from a population driven by latent structures. This modeling choice treats the orientations of the view-specific projections as generic, thereby avoiding worst-case geometric configurations. For this random scenario, we assume \mathbf{V}_k is sign symmetric conditional on \mathbf{W}_k as follows:

Assumption 1. For each $k \in [K]$, \mathbf{V}_k is sign symmetric conditional on \mathbf{W}_k : $(\mathbf{V}_k | \mathbf{W}_k) \stackrel{d}{=} (-\mathbf{V}_k | \mathbf{W}_k)$. Moreover, there exists $\lambda_{k,\min} > 0$, such that with probability exceeding $1 - p_k$, the smallest singular value of $[\mathbf{V}_k \ \mathbf{W}_k]$ is lower bounded by $\lambda_{k,\min}$.

This assumption holds for a broad class of symmetric distributions, such as i.i.d. sub-Gaussian matrices, where random matrix theory guarantees sufficient signal strength via the lower bound on the smallest singular value.

3.2 Equal-weight Case

We begin with the equal weights case. In this case, the misalignment is measured by

$$\theta := 1 - \left\| \frac{1}{K} \sum_{k=1}^K \mathbf{U}_k \mathbf{U}_k^\top \right\|. \quad (5)$$

Notice that $\theta \in [0, 1 - 1/K]$ and θ quantifies the difficulty recovering \mathbf{U} with the presence of individual components. When $\theta = 0$, $\bigcap_{k=1}^K \text{span}(\mathbf{U}_k)$ is non-empty and the joint subspace

$\text{span}(\mathbf{U})$ is not identifiable. When $\theta = 1 - 1/K$, all the individual subspaces $\{\mathbf{U}_k\}_{k=1}^K$ are orthogonal to each other. Intuitively, separating joint from individual subspaces becomes harder as θ approaches 0.

For the equal-weight case, we consider the homogeneous scenario where all views \mathbf{A}_k share similar signal-to-noise ratios (SNR) and dimensionalities. By *homogeneous*, we mean that the SNR_k across the views are comparable, denoted as $\text{SNR}_k \asymp \text{SNR}$, and that the second dimensions of each matrix \mathbf{A}_k satisfy $d_k \asymp d$, for all k . As a result, we have $\varepsilon_k \asymp \varepsilon$, where $\varepsilon := n^{1/2}\text{SNR}^{-1} + (nd)^{1/2}\text{SNR}^{-2}$. However, we make no assumption on the scale δ_k . The following result offers a natural baseline for our algorithm in the equal-weight case with $w_k = 1/K$.

Theorem 1. *Assume*

$$\kappa_k \text{SNR}^{-1} n^{1/2} + \text{SNR}^{-2} (nd)^{1/2} \leq c, \quad \forall k \in [K] \quad \text{and} \quad \theta \geq c \left(\varepsilon^2 + \sqrt{\frac{\log n}{K}} \varepsilon \right),$$

for some universal constant $c > 0$. Then we have with probability exceeding $1 - O(Ke^{-n\wedge d})$, the output of Algorithm 1 with the choice $w_k = 1/K$ for $k \in [K]$ satisfies

$$\|\widehat{\mathbf{U}}\widehat{\mathbf{U}}^\top - \mathbf{U}\mathbf{U}^\top\| \lesssim \varepsilon \sqrt{\frac{\bar{r} \log n}{K} (n^{-1}\theta^{-1} r_{\text{avg}} + 1)} + \varepsilon^2 \theta^{-1} \left(\sqrt{\frac{\log n}{K}} + \frac{\sum_{k=1}^K (\delta_k (1 - \delta_k^2)^{-1} \wedge 1)}{K} \right),$$

where $r_{\text{avg}} := K^{-1} \sum_{k=1}^K r_k$.

Connection with Yang and Ma (2025). For comparison, we first introduce the main results in Yang and Ma (2025), where we assume $r, r_k \asymp 1$ for simplicity. In particular, they consider exact homogeneous noise case where $\sigma_k = \sigma$ for all k , and establish the following bound for $\|\widehat{\mathbf{U}}\widehat{\mathbf{U}}^\top - \mathbf{U}\mathbf{U}^\top\|$:

$$\underbrace{\varepsilon \sqrt{\frac{\log^5 n}{Kn\theta} + \frac{\log^5 n}{K}} + \varepsilon \sqrt{\frac{\log^2 n}{K\theta(K\theta + 1)}}}_{\text{first-order}} + \underbrace{\varepsilon^2 \left(\frac{1}{\theta} + \frac{1}{K\theta^2} \right) \log n}_{\text{second-order}}. \quad (6)$$

Moreover, they established the minimax lower bound of order

$$\varepsilon \sqrt{\frac{1}{Kn\theta} + \frac{1}{K}}. \quad (7)$$

In contrast, Theorem 1 provides the following bound for $\|\widehat{\mathbf{U}}\widehat{\mathbf{U}}^\top - \mathbf{U}\mathbf{U}^\top\|$ under the same assumption on SNR and θ :

$$\underbrace{\varepsilon\sqrt{\frac{\log n}{Kn\theta} + \frac{\log n}{K}}}_{\text{first-order}} + \underbrace{\varepsilon^2\sqrt{\frac{\log n}{K\theta^2}} + \varepsilon^2 \cdot \frac{\sum_{k=1}^K (\delta_k(1 - \delta_k^2)^{-1} \wedge 1)}{K\theta}}_{\text{second-order}}. \quad (8)$$

In light of (6) and (8), our result offers a sharper upper bound. For the first-order term, their bound has an extra term $((K\theta)^{-1} \wedge (K\theta)^{-1/2}) \log n \cdot \varepsilon$, which is not negligible when $K\theta \leq 1$. Moreover, our first-order term in (8) matches the lower bound (7) up to logarithmic factor. For the second-order term, their result has a term $\theta^{-1} \log n \cdot \varepsilon^2$ that does not vanish with K , as their analysis fails to account for the angle between \mathbf{V}_k and \mathbf{W}_k . However, our bound incorporates a specific dependence on δ_k , which can be viewed as more refined characterization of the high-order terms. A special case of particular interest occurs when δ_k are small (e.g., the orthogonal case when $\mathbf{V}_k^\top \mathbf{W}_k = 0$), such that $\sum_{k=1}^K \delta_k(1 - \delta_k^2)^{-1} \lesssim K^{1/2}$. In this case, the second-order term reduces to $(K\theta^2)^{-1/2} \log^{1/2} n \cdot \varepsilon^2$, which vanishes as K goes to infinity. Nonetheless, even if the δ_k are large such that the last term in (8) does not vanish as $K \rightarrow \infty$, our bound remains sharper as we eliminate the extra term $(K\theta^2)^{-1} \log n \cdot \varepsilon$.

The specific dependence on δ_k allows us to derive a vanishing bound for the random-design case, where $\mathbf{V}_k, \mathbf{W}_k$ are assumed to be random.

Theorem 2. *Suppose Assumption 1 holds, and*

$$\kappa_k \text{SNR}^{-1} n^{1/2} + \text{SNR}^{-2} (nd)^{1/2} \leq c, \quad \forall k \in [K] \quad \text{and} \quad \theta \geq c \left(\varepsilon^2 + \varepsilon \sqrt{\frac{\log n}{K}} \right),$$

for some universal constant $c > 0$. Then we have with probability exceeding $1 - O(Ke^{-n\wedge d}) - \sum_{k=1}^K p_k$, the output of Algorithm 1 with the choice $w_k = 1/K$ for $k \in [K]$ satisfies

$$\|\widehat{\mathbf{U}}\widehat{\mathbf{U}}^\top - \mathbf{U}\mathbf{U}^\top\| \lesssim \varepsilon \sqrt{\frac{\bar{r} \log n}{K} (n^{-1}\theta^{-1} r_{\text{avg}} + 1)} + \varepsilon^2 \theta^{-1} \sqrt{\frac{\log n}{K}},$$

where $r_{\text{avg}} = K^{-1} \sum_{k=1}^K r_k$.

In the random-design regime, aggregation across views strictly helps the estimation for joint subspace, whose error decreases with the number of views at the $O(K^{-1/2})$ rate.

When θ is lower bounded by a constant, our upper bound in Theorem 2 essentially matches the minimax lower bound (7) established in Yang and Ma (2025) up to r, r_k and logarithmic factor. In this regime, the estimation error for the joint subspace is comparable to the scenario where no individual components exist. This suggests that the presence of individual components does not impose additional difficulty in recovering the joint subspace. We now discuss a special case to illustrate this phenomenon.

Proposition 1. *Under the setting of Theorem 2, for each k , let \mathbf{U}_k be an independent random matrix sampled uniformly from the set of orthogonal matrices of dimension $n \times r_k$ contained entirely within $\text{span}(\mathbf{U})^\perp$. Also assume $\varepsilon_k \asymp \varepsilon$, $n \geq 4r_{\text{avg}} + r$, $K \geq C \log n$. Then with the choice $w_k = 1/K$ for $k \in [K]$, we have with probability exceeding $1 - n^{-10}$,*

$$\left\| \widehat{\mathbf{U}}\widehat{\mathbf{U}}^\top - \mathbf{U}\mathbf{U}^\top \right\| \lesssim \varepsilon \sqrt{\frac{\bar{r} \log n}{K}}.$$

Connection with Tang et al. (2025). Recently, Tang et al. (2025) proposed a framework for a multi-view spiked covariance model, which can be viewed as a special case of JIVE model (2) with \mathbf{W} also shared across views (implying $r_k = r', d_k = d$). While their data generating process and ours are different and neither strictly subsumes the other, we can compare the theoretical guarantees within the intersection of ours and theirs. In particular, we consider

$$\mathbf{A}_k = \mathbf{U}\mathbf{V}_k^\top + \mathbf{U}_k\mathbf{W}^\top + \mathbf{E}_k.$$

Here, we assume $\{\mathbf{U}_k\}_{k=1}^K$ are generated under the setting of Proposition 1, and \mathbf{V}_k are i.i.d. such that Assumption 1 is satisfied. We further consider $\sigma_k = \sigma$ for $k \in [K]$, $n \asymp d$ and $r, r' \asymp 1$ for simplicity.

In this context, the MOP-UP algorithm in Tang et al. (2025) consists of two stages. The initialization stage is equivalent to Algorithm 1 with equal weights (i.e., AJIVE) and they obtain a bound of $O(\varepsilon^2)$. They subsequently refine this initial estimator via alternating projection to derive a final bound of order $(K^{-1} \log n)^{1/2}$, provided that $K \gtrsim \varepsilon^{-4} \log n$. In comparison, our upper bound is of order $\varepsilon \cdot (K^{-1} \log n)^{1/2}$, merely requiring $K \gtrsim \log n$. As $\varepsilon \asymp n^{1/2} \text{SNR}^{-1} \leq c$ for some small constant $c > 0$, this underscores several key advantages of our analysis. First, our result holds under a much milder condition on the number of views K . Second, in the regime where their condition on K is satisfied, our bound is strictly

smaller than their initialization error. Finally, unlike their refined bound which vanishes as $K \rightarrow \infty$ but is independent of signal strength, our bound vanishes as either $K \rightarrow \infty$ or $\text{SNR} \rightarrow \infty$ and is minimax-optimal. This suggests that in this scenario iterative refinement may be theoretically redundant.

3.3 General-weight Case

The equal-weight choice analyzed in Section 3.2 yields a clean bound in the homogeneous regime. However, in many applications, the view dimensions d_k and the signal-to-noise ratios SNR_k may vary substantially across k , making equal weighting potentially inefficient. Perhaps more surprisingly, as we will see in the next theorem, equal weights need not be optimal even under homogeneity.

A key difference from the equal weight analysis is the notion of misalignment under general weights. For $\mathbf{w} = (w_1, \dots, w_K) \in \Delta_K$ where $\Delta_K := \{\tilde{\mathbf{w}} \in \mathbb{R}^K : \tilde{w}_k \geq 0, \sum_{k=1}^K \tilde{w}_k = 1\}$, we define

$$\theta(\mathbf{w}) := 1 - \left\| \sum_{k=1}^K w_k \mathbf{U}_k \mathbf{U}_k^\top \right\|.$$

The choice of \mathbf{w} directly influences the alignment level of the individual subspaces, offering flexibility to reduce $\theta(\mathbf{w})$ by down-weighting closely aligned views. In the following, we will drop the dependence on \mathbf{w} in the subscript when the context is clear. The following example highlights the importance of weight choice.

Example 2. *Let $r_k = 1$ for all $k \in [K]$, and $\mathbf{u}_1 = \dots = \mathbf{u}_{K-1} = \mathbf{v}$, \mathbf{u}_K is orthogonal to \mathbf{v} . Then with equal weights, we have $\theta(\mathbf{w}) = K^{-1}$. However, if we choose $w_1 = w_K = \frac{1}{2}$ and $w_2 = \dots = w_{K-1} = 0$, $\theta(\mathbf{w}) = \frac{1}{2}$.*

We denote the eigen-decomposition of $\mathbf{I} - \sum_{k=1}^K w_k \bar{\mathbf{U}}_k \bar{\mathbf{U}}_k^\top = \mathbf{U}_\perp \boldsymbol{\Lambda} \mathbf{U}_\perp^\top$ and also recall $\varepsilon_k = n^{1/2} \lambda_{k,\min}^{-1} \sigma_k + (nd_k)^{1/2} \lambda_{k,\min}^{-2} \sigma_k^2$. With these notations in place, we now state the general weights theorem, which quantifies how reweighting interacts with θ and improves upon equal weights.

Theorem 3. Fix $\mathbf{w} \in \Delta_K$. Assume

$$\begin{aligned} \kappa_k \text{SNR}_k^{-1} n^{1/2} + \text{SNR}_k^{-2} (nd_k)^{1/2} &\leq c, \quad \forall k \in [K], \\ \theta &\geq c \cdot \max \left\{ \sum_{k=1}^K w_k \varepsilon_k^2, \left(\sum_{k=1}^K w_k^2 \varepsilon_k^2 \log n \right)^{1/2} \right\}, \end{aligned} \quad (9)$$

for some universal constant $c > 0$. Then we have with probability exceeding $1 - O(\sum_{k=1}^K e^{-n \wedge d_k})$,

$$\begin{aligned} \left\| \widehat{\mathbf{U}} \widehat{\mathbf{U}}^\top - \mathbf{U} \mathbf{U}^\top \right\| &\lesssim \sqrt{\sum_{k=1}^K n^{-1} w_k^2 (\text{tr}(\mathbf{M}_k) + \bar{r}_k \|\mathbf{M}_k\|) \varepsilon_k^2 \sqrt{\log(n)}} \\ &\quad + \sqrt{\sum_{k=1}^K w_k^2 \varepsilon_k^4 \theta^{-2} \sqrt{\log n} + \sum_{k=1}^K w_k (\delta_k (1 - \delta_k^2)^{-1} \wedge 1) \varepsilon_k^2 \theta^{-1}}, \end{aligned}$$

where $\mathbf{M}_k := \bar{\mathbf{U}}_{k\perp}^\top \mathbf{U}_\perp \mathbf{\Lambda}^{-2} \mathbf{U}_\perp^\top \bar{\mathbf{U}}_{k\perp}$.

Crucially, the validity of Theorem 3 relies on satisfying the condition (9), where θ is controlled by the alignment of the individual subspaces $\{\mathbf{U}_k\}_{k=1}^K$, and the right-hand side threshold depends on per-view quality through $\{\varepsilon_k\}_{k=1}^K$. Hence, one can face regimes with small θ (well-aligned individual subspaces) but uneven view quality where some ε_k are small and others are large. In such cases, equal weighting may fail the condition, as illustrated by Example 2, while choosing proper weights can adjust θ to meet the condition (9) as well as improving the overall error bound.

Unlike the equal-weight case, the upper bound in Theorem 3 is also more involved. In particular, it provides a precise characterization of the two layers of heterogeneity introduced earlier. The term ε_k captures the statistical heterogeneity induced by view-specific SNR_k and d_k , while the matrix term \mathbf{M}_k encapsulates the structural heterogeneity driven by the orientation of the individual subspace \mathbf{U}_k relative to null space \mathbf{U}_\perp . Unlike heterogeneous PCA where optimal weights are typically inversely proportional to the SNR Baharav et al. (2025), the JIVE setting presents a more complex scenario due to non-linear dependence of θ and \mathbf{M}_k on the weights $\{w_k\}_{k=1}^K$ themselves. These dependencies explain why a general closed form solution for the optimal weights is intractable.

However, instructive special cases exist where the choice of weights simplifies. First, Proposition 1 highlights that under the constant alignment assumption $\theta \geq c_0$ for some

small absolute constant $c_0 > 0$ and Assumption 1, equal weighting suffices and essentially achieves minimax optimality if statistical heterogeneity is low. Second, in the scenario where individual components are absent ($\mathbf{U}_k = 0$), the structural heterogeneity vanishes entirely. In this case, our upper bound depends solely on the statistical error terms, and minimizing the bound yields a closed form representation for the optimal weights as $w_k \propto \varepsilon_k^{-2}$. As this specific regime serves as a natural benchmark, it is informative to compare our results with recent development in the literature.

Connection with Baharav et al. (2025). Baharav et al. (2025) investigates the performance of weighted versions of SVD-Stack (equivalent to AJIVE) and Stack-SVD in the absence of individual components ($\mathbf{U}_k = 0$). For comparison, we consider the rank-one case $r = 1$ when the joint subspace degenerates to a vector \mathbf{u} and the regime where $\max_{k \in [K]} \varepsilon_k = o(1)$. Assuming the proportional regime where $d_k/n \asymp 1$, they derive the asymptotically optimal weights for SVD-Stack and the corresponding error bound as¹

$$w_k \propto \varepsilon_k^{-2}(1 + o(1)), \quad \|\widehat{\mathbf{u}}\widehat{\mathbf{u}}^\top - \mathbf{u}\mathbf{u}^\top\| \lesssim \frac{n}{\sum_{k=1}^K \text{SNR}_k^4 / (\text{SNR}_k^2 + d_k)}.$$

In other words, our optimal weights and the corresponding bound are asymptotically equivalent to theirs, demonstrating optimality in the absence of individual components. Notably, while the results in Baharav et al. (2025) rely on asymptotic analysis within the proportional regime, our results are non-asymptotic and establish this optimality in a more general high-dimensional setting where d_k can be substantially larger than n .

Next, we discuss the case for randomly generated $\{\mathbf{V}_k, \mathbf{W}_k\}_{k=1}^K$ under Assumption 1.

Theorem 4. Fix $\mathbf{w} \in \Delta_K$. Suppose Assumption 1 holds, and

$$\begin{aligned} \kappa_k \text{SNR}_k^{-1} n^{1/2} + \text{SNR}_k^{-2} (nd_k)^{1/2} &\leq c, \quad \forall k \in [K], \\ \theta &\geq c \cdot \max \left\{ \sum_{k=1}^K w_k \varepsilon_k^2, \left(\sum_{k=1}^K w_k^2 \varepsilon_k^2 \log n \right)^{1/2} \right\}, \end{aligned}$$

¹Note that weights in Baharav et al. (2025) are defined in a slightly different way such that their weights are equivalent to ours after squaring them; we adapt their results to our notation here.

for some universal constant $c > 0$. Then we have with probability exceeding $1 - O(\sum_{k=1}^K e^{-n \wedge d_k}) - \sum_{k=1}^K p_k$,

$$\left\| \widehat{\mathbf{U}}\widehat{\mathbf{U}}^\top - \mathbf{U}\mathbf{U}^\top \right\| \lesssim \sqrt{\sum_{k=1}^K n^{-1} w_k^2 (\text{tr}(\mathbf{M}_k) + \bar{r}_k \|\mathbf{M}_k\|) \varepsilon_k^2 \sqrt{\log n}} + \sqrt{\sum_{k=1}^K w_k^2 \varepsilon_k^4 \theta^{-2} \sqrt{\log n}}.$$

As with the equal-weight case, the random orientation of the loadings allows the last term related to $\{\delta_k\}_{k=1}^K$ in the upper of Theorem 3 vanishes. Since the optimal weights in the general case cannot be derived in closed form, we proceed to Section 4 to develop a data-driven algorithm for selecting them.

4 Data-driven Weighting Scheme

Our analysis in Section 3 focuses on the theoretical guarantees of HeteroJIVE for a given choice of weights $\mathbf{w} = (w_1, \dots, w_K)$ on the simplex. In practice, the weights are not known a priori and must be estimated from the data. In this section we first introduce an oracle-optimal weighting algorithm suggested by Theorem 4, and then describe a data-driven implementation based on a plug-in approximation.

4.1 Oracle-aided Procedure

Algorithm 2 Oracle-optimal weighting scheme

Input: $\{\mathbf{A}_k\}_{k=1}^K$, $\mathbf{w}^{(0)}$, r , $\{r_k\}_{k=1}^K$, $\{\varepsilon_k\}_{k=1}^K$, $\{\mathbf{M}_k(\cdot)\}_{k=1}^K$, $\theta(\cdot)$
for $t = 0, \dots, t_{\max} - 1$ **do**
 Compute $c_k^{(t+1)} := \varepsilon_k^4 [\theta(\mathbf{w}^{(t)})]^{-2} + n^{-1} \varepsilon_k^2 [\text{tr}(\mathbf{M}_k(\mathbf{w}^{(t)})) + \bar{r}_k \|\mathbf{M}_k(\mathbf{w}^{(t)})\|]$ for $k \in [K]$.
 Compute $w_k^{(t+1)} := \frac{(c_k^{(t)})^{-1}}{\sum_{j=1}^K (c_j^{(t)})^{-1}}$ for $k \in [K]$.
end for
Output: $\widehat{\mathbf{w}} := \mathbf{w}^{t_{\max}}$

For illustration, we focus on the loading setting in Assumption 1. In light of Theorem 4,

a natural target is the weight vector that minimizes the following term:

$$J(\mathbf{w}) := \sum_{k=1}^K w_k^2 \{ \varepsilon_k^4 \theta^{-2} + n^{-1} \varepsilon_k^2 [\text{tr}(\mathbf{M}_k) + \bar{r}_k \|\mathbf{M}_k\|] \}.$$

Then we define the oracle weight as

$$\mathbf{w}^* := \arg \min_{\mathbf{w} \in \Delta_K} J(\mathbf{w}),$$

where Δ_K is the K -dimensional probability simplex, ε_k is as in (3), $\bar{r}_k = r + r_k$, and recall

$$\mathbf{M}_k = \bar{\mathbf{U}}_{k\perp}^\top \mathbf{U}_\perp \boldsymbol{\Lambda}^{-2} \mathbf{U}_\perp^\top \bar{\mathbf{U}}_{k\perp},$$

where $\mathbf{U}_\perp \boldsymbol{\Lambda} \mathbf{U}_\perp^\top = \mathbf{I} - \sum_{k=1}^K w_k \bar{\mathbf{U}}_k \bar{\mathbf{U}}_k^\top$, and $\bar{\mathbf{U}}_{k\perp}$ is the orthogonal complement of $\bar{\mathbf{U}}_k = \begin{bmatrix} \mathbf{U} & \mathbf{U}_k \end{bmatrix}$.

The optimization is complicated by the fact that both θ and $\{\mathbf{M}_k\}_{k=1}^K$ depend on w through $\sum_{k=1}^K w_k \bar{\mathbf{U}}_k \bar{\mathbf{U}}_k^\top$. To emphasize this dependence, we write $\theta(\mathbf{w})$ and $\mathbf{M}_k(\mathbf{w})$ in what follows. Direct minimization of $J(\mathbf{w})$ is therefore difficult, but we can construct an iterative reweighting scheme that approximately minimizes $J(\mathbf{w})$.

Suppose for the moment that $\{\varepsilon_k\}_{k=1}^K$, $\theta(\cdot)$ and $\{\mathbf{M}_k(\cdot)\}_{k=1}^K$ are known (oracle setting). Given an iterate \mathbf{w} , define

$$c_k(\mathbf{w}) := \varepsilon_k^4 [\theta(\mathbf{w})]^{-2} + n^{-1} \varepsilon_k^2 [\text{tr}(\mathbf{M}_k(\mathbf{w})) + \bar{r}_k \|\mathbf{M}_k(\mathbf{w})\|], \quad \forall k \in [K]. \quad (10)$$

We then update the weights by $\mathbf{w}^{(t+1)} := T(\mathbf{w}^{(t)})$, where $T : \Delta_K \rightarrow \Delta_K$ and

$$T_k(\mathbf{w}) := \frac{[c_k(\mathbf{w})]^{-1}}{\sum_{j=1}^K [c_j(\mathbf{w})]^{-1}}, \quad k \in [K]. \quad (11)$$

In other words, at t -th iteration step we treat $c_k(\mathbf{w}^{(t)})$ as the current ‘‘cost’’ incurred by view k , and assign new weights inversely proportional to this cost. For reference, we summarize the oracle reweighting scheme in Algorithm 2.

The next proposition formalizes that any positive fixed point of the oracle reweighting map T corresponds to a first-order stationary point of the oracle criterion $J(\mathbf{w})$ over the simplex, whose proof can be found in Section B.5.

Proposition 2. Let $\mathbf{w}^\dagger \in \Delta_K$ be a fixed point of T with $w_k^\dagger > 0$ for $k \in [K]$. Assume that (1) $\theta(\mathbf{w}^\dagger) > 0$, and (2) all positive eigenvalues of $\sum_{k=1}^K w_k^\dagger \mathbf{U}_k \mathbf{U}_k^\top$ are simple. Then \mathbf{w}^\dagger is a $L(\theta_0)$ -stationary point of J under the simplex constraint in the sense that

$$\left\| \text{Proj}_{\mathcal{T}}(\nabla J(\mathbf{w}^\dagger)) \right\|_\infty \leq L(\theta_0) := 4\theta_0^{-3} \max_{k \in [K]} \left\{ \varepsilon_k^4 + 3n^{-1} \varepsilon_k^2 \bar{r}_k \right\},$$

where $\theta_0 := \theta(\mathbf{w}^\dagger)/2$, $\mathcal{T} := \{\mathbf{v} \in \mathbb{R}^K : \mathbf{1}^\top \mathbf{v} = 0\}$, and for any vector $\mathbf{g} \in \mathbb{R}^K$, the orthogonal projection onto \mathcal{T} simply subtracts the average of its coordinates as $\text{Proj}_{\mathcal{T}}(\mathbf{g}) := \mathbf{g} - \mathbf{1}\mathbf{1}^\top \mathbf{g}/K$.

Proposition 2 implies that an interior fixed point of T has a small projected gradient, and can be viewed as an approximate KKT solution for the simplex-constrained problem. In other words, this implies that once the algorithm stabilizes, any local perturbation of the weights within the simplex will yield only a negligible change in the objective function.

4.2 Data-driven Procedure

In practice, we only observe \mathbf{A}_k 's and must estimate $\{\varepsilon_k\}_{k=1}^K$, $\theta(\cdot)$ and $\mathbf{M}_k(\cdot)$ from the data, i.e., estimate $(\mathbf{U}, \{\mathbf{U}_k, \mathbf{V}_k, \mathbf{W}_k\}_{k=1}^K)$. Our proposal is to use the equal-weight HeteroJIVE (i.e., AJIVE) as an initial estimator, construct plug-in estimates of the quantities above, and then run Algorithm 2 with these plug-in maps.

Let $(\widehat{\mathbf{U}}^{(0)}, \{\widehat{\mathbf{U}}_k^{(0)}, \widehat{\mathbf{V}}_k^{(0)}, \widehat{\mathbf{W}}_k^{(0)}\}_{k=1}^K)$ be the output of the equal-weight HeteroJIVE (AJIVE). For each $k \in [K]$, define

$$\widehat{\mathbf{U}}_k^{(0)} := \begin{bmatrix} \widehat{\mathbf{U}}^{(0)} & \widehat{\mathbf{U}}_k^{(0)} \end{bmatrix}, \quad \widehat{\mathbf{U}}_{k\perp}^{(0)} \widehat{\mathbf{U}}_{k\perp}^{(0)\top} := \mathbf{I} - \widehat{\mathbf{U}}_k^{(0)} \widehat{\mathbf{U}}_k^{(0)\top},$$

and let $\widehat{\mathbf{U}}_\perp^{(0)} \widehat{\mathbf{\Lambda}}^{(0)} \widehat{\mathbf{U}}_\perp^{(0)\top}$ be the rank $n - r$ decomposition of $\mathbf{I} - K^{-1} \sum_{k=1}^K \widehat{\mathbf{U}}_k^{(0)} \widehat{\mathbf{U}}_k^{(0)\top}$. In addition, let $\widehat{\lambda}_{k,\min}^{(0)}$ be the $r+r_k$ -th largest singular value of $\widehat{\mathbf{A}}_k^{(0)} := \widehat{\mathbf{U}}^{(0)} \widehat{\mathbf{V}}_k^{(0)\top} + \widehat{\mathbf{U}}_k^{(0)} \widehat{\mathbf{W}}_k^{(0)\top}$, and define

$$\widehat{\sigma}_k^{(0)} := \frac{\|\mathbf{A}_k - \widehat{\mathbf{A}}_k^{(0)}\|_F}{\sqrt{nd_k - (r+r_k)(n+d_k-r-r_k)}}.$$

We then construct plug-in estimates

$$\begin{aligned}\widehat{\mathbf{M}}_k^{(0)} &:= \widehat{\mathbf{U}}_{k\perp}^{(0)\top} \widehat{\mathbf{U}}_{\perp}^{(0)} (\widehat{\boldsymbol{\Lambda}}^{(0)})^{-2} \widehat{\mathbf{U}}_{\perp}^{(0)\top} \widehat{\mathbf{U}}_{k\perp}^{(0)}, & \widehat{\theta}^{(0)} &:= 1 - \left\| K^{-1} \sum_{k=1}^K \widehat{\mathbf{U}}_k^{(0)} \widehat{\mathbf{U}}_k^{(0)\top} \right\|, \\ \widehat{\varepsilon}_k^{(0)} &:= \sqrt{n} (\widehat{\text{SNR}}_k^{(0)})^{-1} + \sqrt{nd_k} (\widehat{\text{SNR}}_k^{(0)})^{-2}, & \widehat{\text{SNR}}_k^{(0)} &:= \widehat{\lambda}_{k,\min} / \widehat{\sigma}_k, \quad \forall k \in [K].\end{aligned}$$

Conceptually, $\widehat{\mathbf{M}}_k^{(0)}$ and $\widehat{\theta}^{(0)}$ can be viewed as evaluations of empirical maps

$$\widehat{\mathbf{M}}_k(\cdot) : \mathbb{R}^K \rightarrow \mathbb{R}^{n \times (n - \bar{r}_k)}, \quad \widehat{\theta}(\cdot) : \mathbb{R}^K \rightarrow \mathbb{R},$$

at the initial weight $\mathbf{w}^{(0)} = K^{-1} \mathbf{1}_K$, i.e., $\widehat{\mathbf{M}}_k^{(0)} \equiv \widehat{\mathbf{M}}_k(\mathbf{w}^{(0)})$ and $\widehat{\theta}^{(0)} \equiv \widehat{\theta}(\mathbf{w}^{(0)})$.

In the data-driven scheme, we replace $\{\varepsilon_k, \mathbf{M}_k(\cdot), \theta(\cdot)\}$ in Algorithm 2 by $\{\widehat{\varepsilon}_k^{(0)}, \widehat{\mathbf{M}}_k(\cdot), \widehat{\theta}(\cdot)\}$ constructed above, initialize $\mathbf{w}^{(0)}$ as equal weights, and run a small number of reweighting iterations to obtain $\widehat{\mathbf{w}}$. Serving as a coarse initial approximation, the plug-in quantities $\{\widehat{\varepsilon}_k^{(0)}, \widehat{\mathbf{M}}_k(\cdot), \widehat{\theta}(\cdot)\}$ are typically close to their oracle counterparts. Empirically, we observe Algorithm 2 converges in a few iterations. The final estimate $\widehat{\mathbf{w}}$ is then used as the weight vector in HeteroJIVE.

5 Numerical Experiments

We consider the following reparameterization of JIVE model:

$$\mathbf{A}_k = s_k (\mathbf{U} \mathbf{V}_k^\top + \gamma \mathbf{U}_k \mathbf{W}_k^\top) + \mathbf{E}_k.$$

where \mathbf{E}_k has i.i.d. $N(0, \sigma_k^2)$ entries. Here s_k controls the overall signal strength, and γ controls the signal strength for the individual loading. Throughout this section, we set $s = s_1 = \dots = s_K$, $r = r_1 = \dots = r_K$ and $d = d_1 = \dots = d_K$, with $d > 2r$.

For generating \mathbf{U} and $\{\mathbf{U}_k\}_{k=1}^K$, we consider a similar procedure to that in Yang and Ma (2025). In particular, we sample the shared subspace \mathbf{U} randomly from $\mathcal{O}_{n,r}$. For the individual subspace $\{\mathbf{U}_k\}_{k=1}^K$, we construct

$$\mathbf{U}_k = \sqrt{1 - \theta} \mathbf{Z} + \sqrt{\theta} \mathbf{Z}_k, \quad \forall k \in [K].$$

Here $\mathbf{Z} \in \mathbb{R}^{n \times r}$ is a random orthonormal matrix drawn from $\text{span}(\mathbf{I}_n - \mathbf{U} \mathbf{U}^\top)$, and $\mathbf{Z}_k \in \mathbb{R}^{n \times r}$ is a random orthonormal matrix drawn from $\text{span}(\mathbf{I}_n - \mathbf{U} \mathbf{U}^\top - \mathbf{Z} \mathbf{Z}^\top)$. For the loading matrices \mathbf{V}_k and \mathbf{W}_k , we consider the following generative schemes:

- (Random scheme) Generate \mathbf{V}_k and \mathbf{W}_k independently randomly from $\mathbb{O}_{d,r}$ for each $k \in [K]$.
- (Shared scheme) Generate \mathbf{V} and \mathbf{W} independently randomly from $\mathbb{O}_{d,r}$, and let $\mathbf{V}_k = \mathbf{V}$ and $\mathbf{W}_k = \mathbf{W}$ for each $k \in [K]$.
- (Shared-orthogonal scheme) Generate $\mathbf{Q} = [\mathbf{q}_1, \dots, \mathbf{q}_d]$ randomly from \mathbb{O}_d , and let $\mathbf{V}_k = [\mathbf{q}_1, \dots, \mathbf{q}_r]$ and $\mathbf{W}_k = [\mathbf{q}_{r+1}, \dots, \mathbf{q}_{2r}]$ for each $k \in [K]$.
- (Random-orthogonal scheme) Generate $\mathbf{Q}_k = [\mathbf{q}_{k,1}, \dots, \mathbf{q}_{k,d}]$ randomly from \mathbb{O}_d , and let $\mathbf{V}_k = [\mathbf{q}_{k,1}, \dots, \mathbf{q}_{k,r}]$ and $\mathbf{W}_k = [\mathbf{q}_{k,r+1}, \dots, \mathbf{q}_{k,2r}]$ for each $k \in [K]$.

Unless otherwise stated, we measure the subspace error $\|\widehat{\mathbf{U}}\widehat{\mathbf{U}}^\top - \mathbf{U}\mathbf{U}^\top\|$ between the estimated and true joint projection matrices (using the operator norm) as a function of \sqrt{K} . For each configuration of $(n, d, r, s, \gamma, \theta, \{\sigma_k\}_{k=1}^K)$ and loading scheme, we repeat the experiment over 100 independent replications and plot the average error across replicates.

5.1 Homogeneous Setting

We first consider a homogeneous setting with identical noise levels across views. In this case, we set $s = 1$, $\sigma = \sigma_1 = \dots = \sigma_K = 1$, $r = 2$ and $n = d = 20$. Since all views share the same noise level, the equal-weight version of HeteroJIVE coincides with AJIVE.

The left panel of Figure 2 compares AJIVE under the four loading schemes described above, with $(\sigma, \theta, \gamma) = (0.1, 0.5, 0.5)$. The simulations confirm the theoretical picture:

- When the loadings are shared and non-orthogonal (shared scheme), the error curve flattens out as K grows, exhibiting the non-vanishing behavior predicted in the low-SNR regime.
- As soon as either randomness across views (random scheme) or orthogonality between \mathbf{V}_k and \mathbf{W}_k (shared-orthogonal and random-orthogonal schemes) is introduced, the cross term is effectively averaged out, and the error decays roughly at the $K^{-1/2}$ rate.

This illustrates that the unfavorable low-SNR phenomenon is not universal: it is tied to a specific configuration where loadings are shared and strongly aligned.

Next, in the right panel of Figure 2 we compare AJIVE to Stack-SVD under the homogeneous setting, using the random loading scheme and $(\sigma, \theta, \gamma) = (0.1, 0.5, 1.5)$. Stack-SVD is implemented by vertically stacking the views and performing PCA on the stacked matrix. The results show that AJIVE consistently achieves lower subspace error than Stack-SVD as K increases. This is consistent with the fact that Stack-SVD does not disentangle joint and individual variation when the relative signal for individual components is strong ($\gamma = 1.5$).

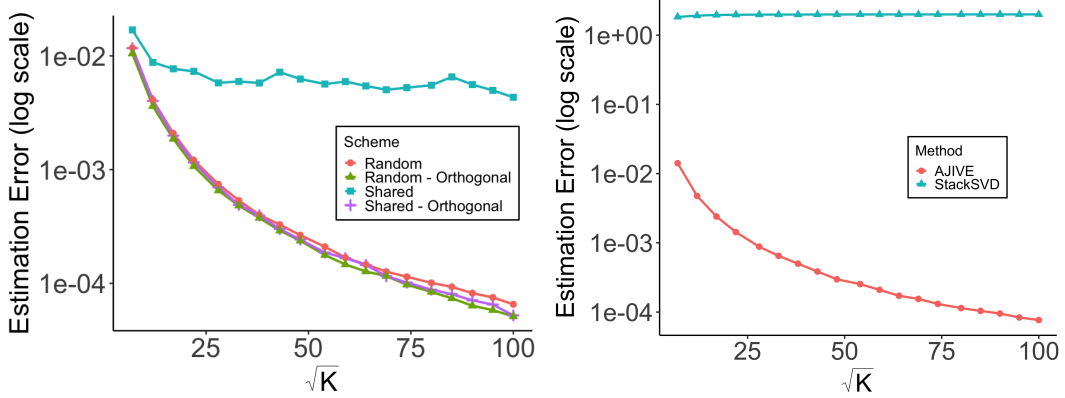


Figure 2: (Performance of AJIVE) Estimation error of $\|\widehat{U}\widehat{U}^\top - UU^\top\|$ versus \sqrt{K} . Comparison across different loading schemes under the homogeneous setting (left) with $\sigma = 0.1$, $\theta = 0.5$ and $\gamma = 0.5$. Comparison with Stack-SVD under the homogeneous setting and random loading scheme (right) with $\sigma = 0.1$, $\theta = 0.5$ and $\gamma = 1.5$.

5.2 Heterogeneous Setting

We now turn to a heterogeneous setting with view-specific noise levels. In this case we set $s = 10$, $\gamma = 2$, $r = 3$ and $n = 40, d = 50$ and draw $\sigma_k \sim \text{Unif}(0.1, 1)$ independently for each $k \in [K]$. We consider both the random loading scheme and the shared-orthogonal scheme, and compare HeteroJIVE with AJIVE and Stack-SVD. Note that for HeteroJIVE, the weights \widehat{w} are learned from the data using the plug-in weighting scheme of Section 4.

Figure 3 reports the results under two loading schemes. Across both panels, HeteroJIVE uniformly outperforms AJIVE and Stack-SVD. Its estimation error decreases roughly at a $K^{-1/2}$ -type rate, and the gap between HeteroJIVE and AJIVE widens as K grows, reflecting the benefit of down-weighting high-noise views in the heterogeneous setting.

Stack-SVD, in contrast, shows almost no improvement with increasing K and remains at a substantially higher error level due to the high relative signal strength for individual components.

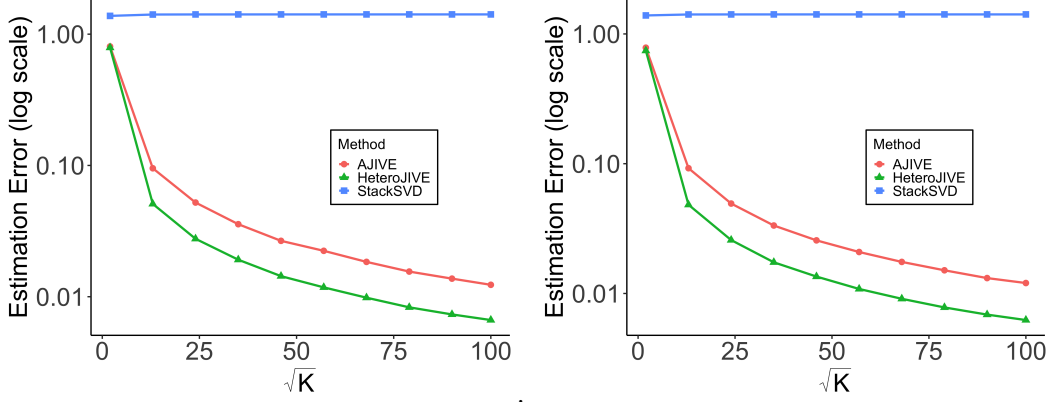


Figure 3: (Comparison across methods under the heterogeneous setting) Estimation error of $\|\widehat{U}\widehat{U}^\top - UU^\top\|$ versus \sqrt{K} with (left) random loading scheme and (right) shared-orthogonal loading scheme. $\sigma_k \stackrel{i.i.d.}{\sim} \text{Unif}(0.1, 2)$, $\theta = 0.6$ and $\gamma = 2$

6 Real-data Analysis

We illustrate HeteroJIVE on the TCGA-BRCA multi-omics dataset with four views: gene expression (GE), DNA methylation (ME), miRNA expression (miRNA), and reverse phase protein array (RPPA). The original data are publicly available from NCI’s Genomic Data Commons and were analyzed in [Network \(2012\)](#). Following the preprocessing procedure in [Lock and Dunson \(2013\)](#), we obtain $K = 4$ datasets on a common set of $n = 348$ tumor samples, including GE data for $d_1 = 645$ genes denoted by $\mathbf{X}_1 \in \mathbb{R}^{348 \times 645}$, ME data for $d_2 = 574$ probes denoted by $\mathbf{X}_2 \in \mathbb{R}^{348 \times 574}$, miRNA data for $d_3 = 423$ miRNAs denoted by $\mathbf{X}_3 \in \mathbb{R}^{348 \times 423}$ and RPPA data for $d_4 = 171$ proteins denoted by $\mathbf{X}_4 \in \mathbb{R}^{348 \times 171}$.

For evaluation, we consider 4 consensus molecular subtypes identified by the multi-source clustering analysis in ([Network, 2012](#)) and further investigated by [Lock and Dunson \(2013\)](#); [Gaynanova and Li \(2019\)](#), which are known to be clinically relevant for prognosis and targeted therapies.

We apply AJIVE and HeteroJIVE on $\{\mathbf{X}_k\}_{k=1}^4$ with ranks fixed at $(r, r_1, r_2, r_3, r_4) = (3, 34, 31, 30, 22)$. These ranks are determined by R package `r.jive` (O’Connell and Lock, 2016) using its default permutation-based procedure and are kept the same for both methods. This yields AJIVE estimates $(\hat{\mathbf{U}}^A, \{\hat{\mathbf{U}}_k^A\}_{k=1}^4)$ and HeteroJIVE estimates $(\hat{\mathbf{U}}^H, \{\hat{\mathbf{U}}_k^H\}_{k=1}^4)$ for the joint and individual subspaces. The data-driven weighting scheme in Section 4 produces $(w_1, w_2, w_3, w_4) = (0.614, 0.053, 0.244, 0.089)$ for HeteroJIVE, placing substantial weight on the GE and miRNA views and downweighting ME and RPPA. In Figure 4, we plot $\hat{\mathbf{U}}^A$ and $\hat{\mathbf{U}}^H$ for visual comparison, and the joint subspaces estimated by HeteroJIVE and AJIVE have broadly similar geometric structures, though the estimated subspaces are not identical as $\|\hat{\mathbf{U}}^H(\hat{\mathbf{U}}^H)^\top - \hat{\mathbf{U}}^A(\hat{\mathbf{U}}^A)^\top\| = 0.3251$.

To complement the visualization and further quantify the performance of AJIVE and HeteroJIVE, we calculate the SWISS score (Cabanski et al., 2010), which measures how well Euclidean distances in the low-dimensional representation align with the a priori subtype labels (lower is better). The SWISS score is 0.5547 for AJIVE and 0.5415 for HeteroJIVE. As a downstream task, we also compute the misclassification rate when clustering samples based on $\hat{\mathbf{U}}^A$ and $\hat{\mathbf{U}}^H$, obtaining an error of 0.3103 for AJIVE and 0.2759 for HeteroJIVE. Both metrics indicate a modest but consistent improvement of HeteroJIVE over AJIVE on this dataset.

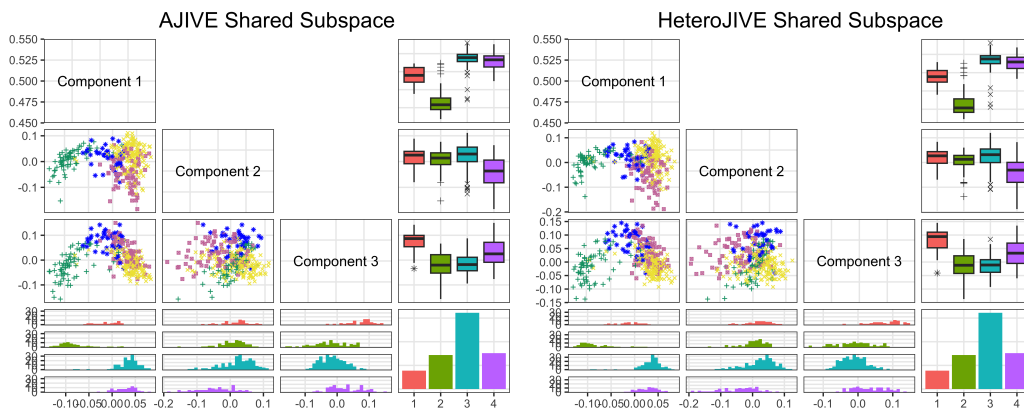


Figure 4: The scatter plots are color-coded by predefined subtypes through consensus clustering analysis in Network (2012).

References

- Jesús Arroyo, Avanti Athreya, Joshua Cape, Guodong Chen, Carey E Priebe, and Joshua T Vogelstein. Inference for multiple heterogeneous networks with a common invariant subspace. *Journal of Machine Learning Research*, 22(142):1–49, 2021.
- Tavor Z Baharav, Phillip B Nicol, Rafael A Irizarry, and Rong Ma. Stacked svd or svd stacked? a random matrix theory perspective on data integration. *arXiv preprint arXiv:2507.22170*, 2025.
- Christopher R Cabanski, Yuan Qi, Xiaoying Yin, Eric Bair, Michele C Hayward, Cheng Fan, Jianying Li, Matthew D Wilkerson, JS Marron, Charles M Perou, et al. Swiss made: Standardized within class sum of squares to evaluate methodologies and dataset elements. *PloS one*, 5(3):e9905, 2010.
- Holger Caesar, Varun Bankiti, Alex H Lang, Sourabh Vora, Venice Erin Liong, Qiang Xu, Anush Krishnan, Yu Pan, Giancarlo Baldan, and Oscar Beijbom. nuscenes: A multimodal dataset for autonomous driving. In *Proceedings of the IEEE/CVF conference on computer vision and pattern recognition*, pages 11621–11631, 2020.
- T Tony Cai and Anru Zhang. Rate-optimal perturbation bounds for singular subspaces with applications to high-dimensional statistics. *The Annals of Statistics*, 46(1):60–89, 2018.
- Jianqing Fan, Dong Wang, Kaizheng Wang, and Ziwei Zhu. Distributed estimation of principal eigenspaces. *Annals of statistics*, 47(6):3009, 2019.
- Qing Feng, Meilei Jiang, Jan Hannig, and JS Marron. Angle-based joint and individual variation explained. *Journal of multivariate analysis*, 166:241–265, 2018.
- Irina Gaynanova and Gen Li. Structural learning and integrative decomposition of multi-view data. *Biometrics*, 75(4):1121–1132, 2019.
- Andreas Geiger, Philip Lenz, Christoph Stiller, and Raquel Urtasun. Vision meets robotics: The kitti dataset. *The international journal of robotics research*, 32(11):1231–1237, 2013.

- Andreas Grammenos, Rodrigo Mendoza Smith, Jon Crowcroft, and Cecilia Mascolo. Federated principal component analysis. *Advances in neural information processing systems*, 33:6453–6464, 2020.
- David Hong, Fan Yang, Jeffrey A Fessler, and Laura Balzano. Optimally weighted pca for high-dimensional heteroscedastic data. *SIAM Journal on Mathematics of Data Science*, 5(1):222–250, 2023.
- Tosio Kato. *Perturbation theory for linear operators*, volume 132. Springer Science & Business Media, 2013.
- Jingyang Li, T Tony Cai, Dong Xia, and Anru R Zhang. Federated pca and estimation for spiked covariance matrices: Optimal rates and efficient algorithm. *arXiv preprint arXiv:2411.15660*, 2024.
- Yingyu Liang, Maria-Florina F Balcan, Vandana Kanchanapally, and David Woodruff. Improved distributed principal component analysis. *Advances in neural information processing systems*, 27, 2014.
- Eric F Lock and David B Dunson. Bayesian consensus clustering. *Bioinformatics*, 29(20):2610–2616, 2013.
- Eric F Lock, Katherine A Hoadley, James Stephen Marron, and Andrew B Nobel. Joint and individual variation explained (jive) for integrated analysis of multiple data types. *The annals of applied statistics*, 7(1):523, 2013.
- Tommy Löfstedt, Daniel Hoffman, and Johan Trygg. Global, local and unique decompositions in onpls for multiblock data analysis. *Analytica chimica acta*, 791:13–24, 2013.
- Zhengchi Ma and Rong Ma. Optimal estimation of shared singular subspaces across multiple noisy matrices. *arXiv preprint arXiv:2411.17054*, 2024.
- The Cancer Genome Atlas Network. Comprehensive molecular portraits of human breast tumours. *Nature*, 490(7418):61–70, 2012.
- Shigeyuki Oba, Motoaki Kawanabe, Klaus-Robert Müller, and Shin Ishii. Heterogeneous component analysis. *Advances in Neural Information Processing Systems*, 20, 2007.

- Michael J O’Connell and Eric F Lock. R. jive for exploration of multi-source molecular data. *Bioinformatics*, 32(18):2877–2879, 2016.
- Claudio Procesi. The invariant theory of $n \times n$ matrices. *Advances in mathematics*, 19(3): 306–381, 1976.
- Renat Sergazinov, Armeen Taeb, and Irina Gaynanova. A spectral method for multi-view subspace learning using the product of projections. *arXiv preprint arXiv:2410.19125*, 2024.
- Naichen Shi and Raed Al Kontar. Personalized pca: Decoupling shared and unique features. *Journal of machine learning research*, 25(41):1–82, 2024.
- Age K Smilde, Johan A Westerhuis, and Sijmen De Jong. A framework for sequential multi-block component methods. *Journal of Chemometrics: A Journal of the Chemometrics Society*, 17(6):323–337, 2003.
- Runshi Tang, Ming Yuan, and Anru R Zhang. Mode-wise principal subspace pursuit and matrix spiked covariance model. *Journal of the Royal Statistical Society Series B: Statistical Methodology*, 87(1):232–255, 2025.
- Roman Vershynin. *High-dimensional probability: An introduction with applications in data science*, volume 47. Cambridge university press, 2018.
- Dong Xia. Normal approximation and confidence region of singular subspaces. *Electronic Journal of Statistics*, 15(2):3798–3851, 2021.
- Yuling Yan, Yuxin Chen, and Jianqing Fan. Inference for heteroskedastic pca with missing data. *The Annals of Statistics*, 52(2):729–756, 2024.
- Yuepeng Yang and Cong Ma. Estimating shared subspace with ajive: the power and limitation of multiple data matrices. *arXiv preprint arXiv:2501.09336*, 2025.
- Anru R Zhang, T Tony Cai, and Yihong Wu. Heteroskedastic pca: Algorithm, optimality, and applications. *The Annals of Statistics*, 50(1):53–80, 2022.
- Yunfeng Zhang and Irina Gaynanova. Joint association and classification analysis of multi-view data. *Biometrics*, 78(4):1614–1625, 2022.

Runbing Zheng and Minh Tang. Limit results for distributed estimation of invariant subspaces in multiple networks inference and pca. *arXiv preprint arXiv:2206.04306*, 2022.

Guoxu Zhou, Andrzej Cichocki, Yu Zhang, and Danilo P Mandic. Group component analysis for multiblock data: Common and individual feature extraction. *IEEE transactions on neural networks and learning systems*, 27(11):2426–2439, 2015.

Supplementary Material to “HeteroJIVE: Joint Subspace Estimation for Heterogeneous Multi-View Data”

This Supplementary Material collects the detailed technical proofs and derivations that support the main results in “HeteroJIVE: Joint Subspace Estimation for Heterogeneous Multi-View Data”.

A Summary

This appendix is organized as follows. First, we present a generalized result, Theorem 5, which encompasses Theorems 1–4. The proofs of our main theorems and propositions are collected in Section B. We provide detailed proofs only on the general weight settings, as the results in Theorems 1 and 2 follow directly as special cases with equal weights. Specifically, the proofs for Theorem 3 and Theorem 4 are located in Section B.1 and Section B.2, respectively. Finally, proofs of the primary lemmas used in Section B are provided in Section C, while additional technical lemmas are deferred to Section D.

We briefly highlight the technical novelty of our analysis. Our primary tool is the explicit representation of the spectral projector developed by Xia (2021). While Yang and Ma (2025) utilizes the same tool, their analysis is restricted to the first-order expansion. Consequently, their derived error bound remains non-vanishing with respect to K , even in the ideal scenario where $\mathbf{V}_k^\top \mathbf{W}_k = 0$. In contrast, our analysis systematically accounts for the full expansion to all orders, which is technically more involved and leads to sharper bounds that can vanish as $K \rightarrow \infty$ under generic geometric conditions.

B Proofs of Theorems and Propositions

We now state the general theorem, whose proof can be found in Section B.3. Recall the misalignment is defined as

$$\theta = 1 - \left\| \sum_{k=1}^K w_k \mathbf{U}_k \mathbf{U}_k^\top \right\|,$$

and $\mathbf{I} - \sum_{k=1}^K w_k \bar{\mathbf{U}}_k \bar{\mathbf{U}}_k^\top = \mathbf{U}_\perp \boldsymbol{\Lambda} \mathbf{U}_\perp^\top$ and $\varepsilon_k = n^{1/2} \lambda_{k,\min}^{-1} \sigma_k + (nd_k)^{1/2} \lambda_{k,\min}^{-2} \sigma_k^2$.

Theorem 5. *Assume*

$$\kappa_k \text{SNR}_k^{-1} n^{1/2} + \text{SNR}_k^{-2} (nd_k)^{1/2} \lesssim 1, \quad \forall k \in [K], \quad (12)$$

$$\theta \gtrsim \max \left\{ \sum_{k=1}^K w_k \varepsilon_k^2, \left(\sum_{k=1}^K w_k^2 \varepsilon_k^2 \log n \right)^{1/2} \right\}. \quad (13)$$

Then we have with probability exceeding $1 - C \sum_{k=1}^K e^{-n \wedge d_k}$,

$$\begin{aligned} \left\| \widehat{\mathbf{U}} \widehat{\mathbf{U}}^\top - \mathbf{U} \mathbf{U}^\top \right\| &\leq C \sqrt{\sum_{k=1}^K n^{-1} w_k^2 (\text{tr}(\mathbf{M}_k) + \bar{r}_k \|\mathbf{M}_k\|) \varepsilon_k^2 \sqrt{\log(n)}} \\ &\quad + C \sqrt{\sum_{k=1}^K w_k^2 \varepsilon_k^4 \theta^{-2} \sqrt{\log n}} + \left\| \sum_{k=1}^K w_k \sum_{r \geq 1} c_{k,r} \mathbf{U}^\top \bar{\mathbf{U}}_k \boldsymbol{\Gamma}_k^{-r} \bar{\mathbf{U}}_k^\top \mathbf{U}_\perp \boldsymbol{\Lambda}^{-1} \right\|, \end{aligned}$$

where $\mathbf{M}_k = \bar{\mathbf{U}}_{k\perp}^\top \mathbf{U}_\perp \boldsymbol{\Lambda}^{-2} \mathbf{U}_\perp^\top \bar{\mathbf{U}}_{k\perp}$, $\boldsymbol{\Gamma}_k = \begin{bmatrix} \mathbf{V}_k^\top \\ \mathbf{W}_k^\top \end{bmatrix} \begin{bmatrix} \mathbf{V}_k & \mathbf{W}_k \end{bmatrix}$, and $c_{k,r}$ satisfy

$$\sum_{r \geq 1} |c_{k,r}| (2\lambda_{k,\min}^{-2})^r \leq C \varepsilon_k^2.$$

B.1 Proof of Theorem 3

It suffices to bound the last term in Theorem 5. First, a trivial bound for $\left\| \mathbf{U}^\top \bar{\mathbf{U}}_k \boldsymbol{\Gamma}_k^{-r} \bar{\mathbf{U}}_k^\top \mathbf{U}_\perp \boldsymbol{\Lambda}^{-1} \right\|$ gives

$$\left\| \mathbf{U}^\top \bar{\mathbf{U}}_k \boldsymbol{\Gamma}_k^{-r} \bar{\mathbf{U}}_k^\top \mathbf{U}_\perp \boldsymbol{\Lambda}^{-1} \right\| \leq \lambda_{k,\min}^{-2r} \theta^{-1}.$$

And this gives the first upper bound.

On the other hand, recall $\boldsymbol{\Gamma}_k = \begin{bmatrix} \mathbf{V}_k^\top \\ \mathbf{W}_k^\top \end{bmatrix} \begin{bmatrix} \mathbf{V}_k & \mathbf{W}_k \end{bmatrix}$, and also notice $\mathbf{U}^\top \bar{\mathbf{U}}_k = \begin{bmatrix} \mathbf{I} & \mathbf{0} \end{bmatrix}$,

and $\bar{\mathbf{U}}_k^\top \mathbf{U}_\perp = \begin{bmatrix} \mathbf{0} \\ \mathbf{U}_k^\top \mathbf{U}_\perp \end{bmatrix}$. From Lemma 11, we conclude

$$\left\| \mathbf{U}^\top \bar{\mathbf{U}}_k \boldsymbol{\Gamma}_k^{-r} \bar{\mathbf{U}}_k^\top \mathbf{U}_\perp \boldsymbol{\Lambda}^{-1} \right\| \leq \left\| [\boldsymbol{\Gamma}_k^{-r}]_{12} \right\| \leq r \lambda_{k,\min}^{-2r} \delta_k (1 - \delta_k^2)^{-1} \theta^{-1},$$

where $[\mathbf{\Gamma}_k^{-r}]_{12}$ is the $(1, 2)$ -th sub-matrix of $\mathbf{\Gamma}_k^{-r}$. Therefore

$$\left\| \sum_{r \geq 1} c_{k,r} \mathbf{U}^\top \bar{\mathbf{U}}_k \mathbf{\Gamma}_k^{-r} \bar{\mathbf{U}}_k^\top \mathbf{U}_\perp \mathbf{\Lambda}^{-1} \right\| \leq C \varepsilon_k^2 (\delta_k (1 - \delta_k^2)^{-1} \wedge 1) \theta^{-1}.$$

And this finishes the proof.

B.2 Proof of Theorem 4

We denote the event $\mathcal{F}_k = \left\{ \lambda_{r+r_k}(\begin{bmatrix} \mathbf{V}_k & \mathbf{W}_k \end{bmatrix}) \geq \lambda_{k,\min} \right\}$. Then by Assumption, $\mathbb{P}(\mathcal{F}_k) \geq 1 - p_k$. Then we have under \mathcal{F}_k , $\begin{bmatrix} \mathbf{V}_k & \mathbf{W}_k \end{bmatrix}$ has full column rank. We now show for any integer $r > 0$,

$$\mathbb{E}[\mathbf{\Gamma}_k^{-r}]_{12} \cdot \mathbf{1}(\mathcal{F}_k) = 0. \quad (14)$$

Under Assumption 1, $(-\mathbf{V}_k | \mathbf{W}_k)$ has the same distribution as $(\mathbf{V}_k | \mathbf{W}_k)$ and thus we prove (14) conditioned on \mathbf{W}_k . We denote $f_{ij}(\mathbf{V}_k) = [\mathbf{\Gamma}_k^{-1}]_{ij}$ for $i, j = 1, 2$. By Schur complement, we see

$$f_{12}(\mathbf{V}_k) := [\mathbf{\Gamma}_k^{-1}]_{12} = -(\mathbf{V}_k^\top \mathbf{V}_k)^{-1} \mathbf{V}_k^\top \mathbf{W}_k (\mathbf{W}_k^\top \mathbf{W}_k - \mathbf{W}_k^\top \mathbf{V}_k (\mathbf{V}_k^\top \mathbf{V}_k)^{-1} \mathbf{V}_k^\top \mathbf{W}_k)^{-1}.$$

Then we have $f_{12}(\mathbf{V}_k) = -f_{12}(-\mathbf{V}_k)$. Since $f_{21}(\mathbf{V}_k) = f_{12}(\mathbf{V}_k)^\top$, it is also odd in \mathbf{V}_k . On the other hand, f_{11} and f_{22} are even in \mathbf{V}_k . And $g(\mathbf{V}_k) := \mathbf{1}(\mathcal{F}_k)$ satisfies $g(\mathbf{V}_k) = g(-\mathbf{V}_k)$. This is because $\begin{bmatrix} \mathbf{V}_k & \mathbf{W}_k \end{bmatrix}$ has the same singular values as $\begin{bmatrix} -\mathbf{V}_k & \mathbf{W}_k \end{bmatrix} = \begin{bmatrix} -\mathbf{V}_k & \mathbf{W}_k \end{bmatrix} \begin{bmatrix} -\mathbf{I} & 0 \\ 0 & \mathbf{I} \end{bmatrix}$. Then

$$[\mathbf{\Gamma}_k^{-r}]_{12} \cdot \mathbf{1}(\mathcal{F}_k) = \sum_{l_1, \dots, l_{r-1}=1,2} f_{1l_1}(\mathbf{V}_k) \cdots f_{l_{r-1}2}(\mathbf{V}_k) g(\mathbf{V}_k).$$

Each summand is even number of even functions in \mathbf{V}_k and together with the assumption that $(-\mathbf{V}_k | \mathbf{W}_k)$ has the same distribution as $(\mathbf{V}_k | \mathbf{W}_k)$, we conclude each summand has mean zero, which verifies (14).

Now we consider

$$\left\| \sum_{k=1}^K w_k \sum_{r \geq 1} c_{k,r} \mathbf{U}^\top \bar{\mathbf{U}}_k \mathbf{\Gamma}_k^{-r} \bar{\mathbf{U}}_k^\top \mathbf{U}_\perp \mathbf{\Lambda}^{-1} \cdot \mathbf{1}(\mathcal{F}_k) \right\|.$$

We have

$$\left\| \sum_{r \geq 1} c_{k,r} \mathbf{U}^\top \bar{\mathbf{U}}_k \mathbf{\Gamma}_k^{-r} \bar{\mathbf{U}}_k^\top \mathbf{U}_\perp \mathbf{\Lambda}^{-1} \cdot \mathbf{1}(\mathcal{F}_k) \right\| \leq C \varepsilon_k^2 \theta^{-1}.$$

And using matrix Hoeffding inequality, we conclude with probability exceeding $1 - e^{-n}$,

$$\left\| \sum_{k=1}^K w_k \sum_{r \geq 1} c_{k,r} \mathbf{U}^\top \bar{\mathbf{U}}_k \mathbf{\Gamma}_k^{-r} \bar{\mathbf{U}}_k^\top \mathbf{U}_\perp \mathbf{\Lambda}^{-1} \cdot \mathbf{1}(\mathcal{F}_k) \right\| \lesssim \left(\sum_{k=1}^K w_k^2 \varepsilon_k^4 \theta^{-2} \log n \right)^{1/2}.$$

And this finishes the proof.

B.3 Proof of Theorem 5

Under the assumption (13), we have $\theta > 0$ and thus $\left\| \sum_{k=1}^K w_k \mathbf{U}_k \mathbf{U}_k^\top \right\| < 1$. Since $\mathbf{U}_k^\top \mathbf{U} = 0$, we can conclude

$$\mathbf{I} - \sum_{k=1}^K w_k \bar{\mathbf{U}}_k \bar{\mathbf{U}}_k^\top = \mathbf{I} - \mathbf{U} \mathbf{U}^\top - \sum_{k=1}^K w_k \mathbf{U}_k \mathbf{U}_k^\top$$

has rank $n - r$ and has $\mathbf{U}_\perp \mathbf{R}_0$ as its top $n - r$ left singular vectors, where $\mathbf{R}_0 \in \mathbb{O}_{n-r}$ is orthogonal matrix, and its minimal non-zero eigenvalue is θ . On the other hand, $\widehat{\mathbf{U}}_\perp$ is the top $n - r$ left singular vectors of $\mathbf{I} - \sum_{k=1}^K w_k \tilde{\mathbf{U}}_k \tilde{\mathbf{U}}_k^\top$.

Let the rank $n - r$ decomposition of $\mathbf{I} - \sum_{k=1}^K w_k \bar{\mathbf{U}}_k \bar{\mathbf{U}}_k^\top$ be $\mathbf{I} - \sum_{k=1}^K w_k \bar{\mathbf{U}}_k \bar{\mathbf{U}}_k^\top = \mathbf{U}_\perp \mathbf{\Lambda} \mathbf{U}_\perp^\top$ (notice here $\mathbf{\Lambda}$ is not necessarily diagonal). And we denote $\mathbf{Q}_\perp = \mathbf{I} - \mathbf{U}_\perp \mathbf{U}_\perp^\top = \mathbf{U} \mathbf{U}^\top$, $\mathbf{Q}^{-s} = \mathbf{U}_\perp \mathbf{\Lambda}^{-s} \mathbf{U}_\perp^\top$ for $s > 0$, and we denote

$$\mathbf{\Delta} = \left(\mathbf{I} - \sum_{k=1}^K w_k \tilde{\mathbf{U}}_k \tilde{\mathbf{U}}_k^\top \right) - \left(\mathbf{I} - \sum_{k=1}^K w_k \bar{\mathbf{U}}_k \bar{\mathbf{U}}_k^\top \right) = \sum_{k=1}^K w_k \underbrace{(\bar{\mathbf{U}}_k \bar{\mathbf{U}}_k^\top - \tilde{\mathbf{U}}_k \tilde{\mathbf{U}}_k^\top)}_{:= \mathbf{\Delta}_k}. \quad (15)$$

We also denote

$$\begin{bmatrix} \mathbf{G}_k \\ \mathbf{H}_k \end{bmatrix} = \begin{bmatrix} \bar{\mathbf{U}}_k^\top \mathbf{E}_k \\ \bar{\mathbf{U}}_{k\perp}^\top \mathbf{E}_k \end{bmatrix},$$

then $\mathbf{G}_k \in \mathbb{R}^{\bar{r}_k \times d_k}$, $\mathbf{H}_k \in \mathbb{R}^{(n-\bar{r}_k) \times d_k}$. We consider the following events:

$$\mathcal{E}_{k,1} = \left\{ \|\mathbf{G}_k \bar{\mathbf{R}}_k\| \lesssim \sqrt{n \wedge d_k} \sigma_k \right\} \cap \left\{ \|\mathbf{H}_k \bar{\mathbf{R}}_k\| \lesssim \sqrt{n} \sigma_k \right\}, \quad (16)$$

and

$$\begin{aligned} \mathcal{E}_{k,2} = & \left\{ \left\| \mathbf{G}_k \mathbf{G}_k^\top - d_k \sigma_k^2 \mathbf{I} \right\| \lesssim \sqrt{(n \wedge d_k) d_k} \sigma_k^2 \right\} \cap \left\{ \left\| \mathbf{G}_k \mathbf{H}_k^\top \right\| \lesssim \sqrt{n d_k} \sigma_k^2 \right\} \\ & \cap \left\{ \left\| \mathbf{H}_k \mathbf{H}_k^\top - d_k \sigma_k^2 \mathbf{I} \right\| \lesssim (\sqrt{n d_k} + n) \sigma_k^2 \right\}. \end{aligned} \quad (17)$$

We also define $\mathcal{E}_k := \mathcal{E}_{k,1} \cap \mathcal{E}_{k,2}$, $\mathcal{E}_{(i)} := \cap_{k=1}^K \mathcal{E}_{k,i}$ for $i = 1, 2$. Then we have $\mathbb{P}(\mathcal{E}_{(1)} \cap \mathcal{E}_{(2)}) \geq 1 - C \sum_{k=1}^K e^{-n \wedge d_k}$.

We now bound the operator norms $\left\| \sum_{k=1}^K w_k \mathbf{U}^\top \mathbf{\Delta}_k \mathbf{U}_\perp \cdot 1(\mathcal{E}_k) \right\|$, $\left\| \sum_{k=1}^K w_k \mathbf{U}^\top \mathbf{\Delta}_k \mathbf{U} \cdot 1(\mathcal{E}_k) \right\|$, and $\left\| \sum_{k=1}^K w_k \mathbf{U}_\perp^\top \mathbf{\Delta}_k \mathbf{U}_\perp \cdot 1(\mathcal{E}_k) \right\|$, which are building blocks of our analysis.

Lemma 1. *We have*

$$\left\| \sum_{k=1}^K w_k \mathbf{U}^\top \mathbf{\Delta}_k \mathbf{U} \cdot 1(\mathcal{E}_k) \right\| \leq C \sum_{k=1}^K w_k \varepsilon_k^2.$$

With probability exceeding $1 - 4Kn^{-10}$, we have for all $k \in [K]$,

$$\begin{aligned} \left\| \sum_{k=1}^K w_k \mathbf{U}^\top \mathbf{\Delta}_k \mathbf{U}_\perp \cdot 1(\mathcal{E}_k) \right\| & \leq C \sum_{k=1}^K w_k \varepsilon_k^2 + C \left(\sum_{k=1}^K w_k^2 \varepsilon_k^2 \log(n) \right)^{1/2}, \\ \left\| \sum_{k=1}^K w_k \mathbf{U}_\perp^\top \mathbf{\Delta}_k \mathbf{U}_\perp \cdot 1(\mathcal{E}_k) \right\| & \leq C \sum_{k=1}^K w_k \varepsilon_k^2 + C \left(\sum_{k=1}^K w_k^2 \varepsilon_k^2 \log(n) \right)^{1/2}. \end{aligned}$$

As a result, we have

$$\left\| \sum_{k=1}^K w_k \mathbf{\Delta}_k \cdot 1(\mathcal{E}_k) \right\| \leq C \sum_{k=1}^K w_k \varepsilon_k^2 + C \left(\sum_{k=1}^K w_k^2 \varepsilon_k^2 \log(n) \right)^{1/2}. \quad (18)$$

Moreover, with probability exceeding $1 - 2Kn^{-10}$, we have for all $k \in [K]$,

$$\begin{aligned} \left\| \sum_{k=1}^K w_k \mathbf{U}^\top \mathbf{\Delta}_k \mathbf{U}_\perp \mathbf{\Lambda}^{-1} \cdot 1(\mathcal{E}_k) \right\| & \leq C \sqrt{\sum_{k=1}^K n^{-1} w_k^2 (\text{tr}(\mathbf{M}_k) + \bar{r}_k \|\mathbf{M}_k\|) \varepsilon_k^2 \sqrt{\log(n)}} \\ & + C \sqrt{\sum_{k=1}^K w_k^2 \varepsilon_k^4 \theta^{-2} \sqrt{\log n}} + \left\| \sum_{k=1}^K w_k \sum_{r \geq 1} c_{k,r} \mathbf{U}^\top \bar{\mathbf{U}}_k \mathbf{\Gamma}_k^{-r} \bar{\mathbf{U}}_k^\top \mathbf{U}_\perp \mathbf{\Lambda}^{-1} \right\| \end{aligned}$$

for some $c_{k,r}$ satisfying $\sum_{r \geq 1} |c_{k,r}| \lambda_{k,\min}^{-2r} \leq C \varepsilon_k^2$.

From (18) and assumption (13), we have $\left\| \sum_{k=1}^K w_k \mathbf{\Delta}_k \right\| \lesssim \theta$, where θ is the minimal non-zero eigenvalue of $\mathbf{I} - \sum_{k=1}^K w_k \bar{\mathbf{U}}_k \bar{\mathbf{U}}_k^\top$. Then from (Xia, 2021, Theorem 1), we can expand $\widehat{\mathbf{U}}\widehat{\mathbf{U}}^\top - \mathbf{U}\mathbf{U}^\top$ as follows ($\mathbf{\Delta}$ defined in (15)):

$$\begin{aligned} \mathbf{U}\mathbf{U}^\top - \widehat{\mathbf{U}}\widehat{\mathbf{U}}^\top &= (\mathbf{I} - \widehat{\mathbf{U}}\widehat{\mathbf{U}}^\top) - (\mathbf{I} - \mathbf{U}\mathbf{U}^\top) \\ &= \sum_{l \geq 1} \sum_{\mathbf{s} \in \mathbb{S}_l} (-1)^{\|\mathbf{s}\|_0 + 1} \mathbf{M}(s_1) \mathbf{\Lambda}^{-s_1} \underline{\mathbf{M}(s_1)^\top \mathbf{\Delta} \mathbf{M}(s_2)} \cdots \underline{\mathbf{M}(s_l)^\top \mathbf{\Delta} \mathbf{M}(s_{l+1})} \mathbf{\Lambda}^{-s_{l+1}} \mathbf{M}(s_{l+1})^\top, \end{aligned}$$

where $\mathbf{M}(0) = \mathbf{U}$, $\mathbf{M}(s) = \mathbf{U}_\perp$ for $s > 0$, $\mathbb{S}_l = \{\mathbf{s} = (s_1, \dots, s_{l+1}) \in \mathbb{N}^{l+1} : s_1 + \dots + s_{l+1} = 0\}$, and $\mathbf{\Lambda}^{-0} = \mathbf{I}_r$ with slight abuse of notation.

Under (13), there exists $c_1 \in (0, 1/4)$, such that

$$\theta^{-1} \max_{s_1, s_2} \left\| \sum_{k=1}^K w_k \mathbf{M}(s_1)^\top \mathbf{\Delta}_k \mathbf{M}(s_2) \right\| \leq c_1.$$

Then for each $l \geq 1$, $\mathbf{s} \in \mathbb{S}_l$,

$$\mathbf{M}(s_1) \mathbf{\Lambda}^{-s_1} \underline{\mathbf{M}(s_1)^\top \mathbf{\Delta} \mathbf{M}(s_2)} \cdots \underline{\mathbf{M}(s_l)^\top \mathbf{\Delta} \mathbf{M}(s_{l+1})} \mathbf{\Lambda}^{-s_{l+1}} \mathbf{M}(s_{l+1})^\top$$

has the following properties: there exist $1 \leq l_0 \leq l$ such that $s_{l_0} > 0$, $s_{l_0+1} = 0$ or $s_{l_0} = 0$, $s_{l_0+1} > 0$. This guarantees the existence of $\mathbf{U}^\top \mathbf{\Delta} \mathbf{U}_\perp \mathbf{\Lambda}^{-1}$. So

$$\begin{aligned} & \left\| \mathbf{M}(s_1) \mathbf{\Lambda}^{-s_1} \underline{\mathbf{M}(s_1)^\top \mathbf{\Delta} \mathbf{M}(s_2)} \cdots \underline{\mathbf{M}(s_l)^\top \mathbf{\Delta} \mathbf{M}(s_{l+1})} \mathbf{\Lambda}^{-s_{l+1}} \mathbf{M}(s_{l+1})^\top \right\| \cdot \mathbf{1}(\mathcal{E}_{(1)} \cap \mathcal{E}_{(2)}) \\ & \leq \left\| \mathbf{U}^\top \mathbf{\Delta} \mathbf{U}_\perp \mathbf{\Lambda}^{-1} \right\| \cdot \mathbf{1}(\mathcal{E}_{(1)} \cap \mathcal{E}_{(2)}) \left(\max_{s_1, s_2} \left\| \mathbf{M}(s_1)^\top \mathbf{\Delta} \mathbf{M}(s_2) \right\| \theta^{-1} \right)^{l-1} \\ & \leq c_1^{l-1} \left\| \mathbf{U}^\top \mathbf{\Delta} \mathbf{U}_\perp \mathbf{\Lambda}^{-1} \right\| \cdot \mathbf{1}(\mathcal{E}_{(1)} \cap \mathcal{E}_{(2)}). \end{aligned}$$

And we can apply the upper bound in Lemma 1. Together with the fact that $|\mathbb{S}_l| \leq 4^l$, we conclude

$$\begin{aligned} \left\| \widehat{\mathbf{U}}\widehat{\mathbf{U}}^\top - \mathbf{U}\mathbf{U}^\top \right\| \cdot \mathbf{1}(\mathcal{E}_{(1)} \cap \mathcal{E}_{(2)}) & \lesssim \sqrt{\sum_{k=1}^K n^{-1} w_k^2 (\text{tr}(\mathbf{M}_k) + \bar{r}_k \|\mathbf{M}_k\|) \varepsilon_k^2 \sqrt{\log(n)}} \\ & + \sqrt{\sum_{k=1}^K w_k^2 \varepsilon_k^4 \theta^{-2} \sqrt{\log n}} + \left\| \sum_{k=1}^K w_k \sum_{r \geq 1} c_{k,r} \mathbf{U}^\top \bar{\mathbf{U}}_k \mathbf{\Gamma}_k^{-r} \bar{\mathbf{U}}_k^\top \mathbf{U}_\perp \mathbf{\Lambda}^{-1} \right\|. \end{aligned}$$

B.4 Proof of Proposition 1

We first show with high probability, θ is lower bounded by $1/2$. Recall $\theta = 1 - K^{-1} \left\| \sum_{k=1}^K \mathbf{U}_k \mathbf{U}_k^\top \right\|$. From the way \mathbf{U}_k generated, we have $\mathbb{E} \mathbf{U}_k \mathbf{U}_k^\top = r_k / (n - r) \mathbf{I}$. And $\left\| \mathbf{U}_k \mathbf{U}_k^\top - \frac{r_k}{n-r} \mathbf{I} \right\| \leq 1$. On the other hand, $\left\| \mathbb{E} (\mathbf{U}_k \mathbf{U}_k^\top - \frac{r_k}{n-r} \mathbf{I})^2 \right\| \leq r_k / (n - r)$. Using matrix Bernstein inequality, we obtain with probability exceeding $1 - n^{-10}$,

$$\left\| \sum_{k=1}^K \frac{1}{K} \mathbf{U}_k \mathbf{U}_k^\top \right\| \leq \frac{r_{\text{avg}}}{n-r} + C \sqrt{\frac{r_{\text{avg}} \log n}{(n-r)K}} + C \frac{\log n}{K} \leq 1/2,$$

where in the last inequality we use $n \geq 4r' + r$, $K \geq C \log n$. In this case, setting $w_k = 1/K$ gives the upper bound

$$\left\| \widehat{\mathbf{U}} \widehat{\mathbf{U}}^\top - \mathbf{U} \mathbf{U}^\top \right\| \lesssim \sqrt{\frac{\bar{r} \log n}{K}} \varepsilon.$$

B.5 Proof of Proposition 2

Define a ℓ_1 ball around \mathbf{w}^\dagger as

$$\Omega_{\theta_0}(\mathbf{w}^\dagger) := \left\{ \mathbf{w} \in \Delta_K : \left\| \mathbf{w} - \mathbf{w}^\dagger \right\|_1 \leq \theta_0 \right\}.$$

We start with the following two lemmas, whose proofs are deferred to Section C.2 and Section C.3.

Lemma 2. *For any $\mathbf{w}, \mathbf{w}' \in \Omega_{\theta_0}(\mathbf{w}^\dagger)$, we have*

$$\left\| c_k(\mathbf{w}) - c_k(\mathbf{w}') \right\| \leq \frac{L(\theta_0)}{2} \left\| \mathbf{w} - \mathbf{w}' \right\|_1, \quad \forall k \in [K].$$

Lemma 3. *Suppose the conditions of Proposition 2 hold, then there exists a neighborhood Ω of \mathbf{w}^\dagger such that $\{c_k(\mathbf{w})\}_{k=1}^K$ and $J(\mathbf{w})$ are C^1 on Ω .*

We are ready to prove Proposition 2. Since \mathbf{w}^\dagger is a fixed point, then by (11) we get

$$w_k^\dagger = \frac{c_k(\mathbf{w}^\dagger)^{-1}}{\sum_{j=1}^K c_j(\mathbf{w}^\dagger)^{-1}}, \quad k \in [K].$$

Define $\alpha := (\sum_{j=1}^K c_j(\mathbf{w}^\dagger)^{-1})^{-1}$, then we get $w_k^\dagger c_k(\mathbf{w}^\dagger) = \alpha$ for $k \in [K]$. We thus get

$$\frac{\partial J(\mathbf{w}^\dagger)}{\partial w_k} = 2\alpha + \sum_{j=1}^K (w_j^\dagger)^2 \frac{\partial c_j(\mathbf{w}^\dagger)}{\partial w_k}, \quad k \in [K].$$

Then for any $k, l \in [K]$, Lemma 2 implies that

$$\left| \frac{\partial J(\mathbf{w}^\dagger)}{\partial w_k} - \frac{\partial J(\mathbf{w}^\dagger)}{\partial w_l} \right| \leq \sum_{j=1}^K (w_j^\dagger)^2 \left| \frac{\partial c_j(\mathbf{w}^\dagger)}{\partial w_k} - \frac{\partial c_j(\mathbf{w}^\dagger)}{\partial w_l} \right| \leq 2L(\theta_0).$$

Let $S = K^{-1} \sum_{k=1}^K \frac{\partial J(\mathbf{w}^\dagger)}{\partial w_k}$, we thus arrive at

$$\left\| \text{Proj}_{\mathcal{T}} \left(\nabla J(\mathbf{w}^\dagger) \right) \right\|_\infty = \left\| \nabla J(\mathbf{w}^\dagger) - S \mathbf{1}_K \right\|_\infty = \max_k \left| \frac{\partial J(\mathbf{w}^\dagger)}{\partial w_k} - S \right| \leq 2L(\theta_0).$$

C Proofs of Lemmas

C.1 Proof of Lemma 1

We start with the expansion of Δ_k . Recall $\mathbf{A}_k = \underbrace{\mathbf{U}\mathbf{V}_k^\top + \mathbf{U}_k\mathbf{W}_k^\top}_{:=\mathbf{A}_k^*} + \mathbf{E}_k$, and $\bar{\mathbf{U}}_k = \begin{bmatrix} \mathbf{U} & \mathbf{U}_k \end{bmatrix}$ is the top $\bar{r}_k = r + r_k$ left singular vectors of $\mathbf{A}_k^* \mathbf{A}_k^{*\top}$, $\tilde{\mathbf{U}}_k$ is the top \bar{r}_k left singular vectors of $\mathbf{A}_k \mathbf{A}_k^\top - d_k \sigma_k^2 \mathbf{I}$. Then \mathbf{A}_k^* admits a rank \bar{r}_k decomposition as

$$\mathbf{A}_k^* = \begin{bmatrix} \mathbf{U} & \mathbf{U}_k \end{bmatrix} \begin{bmatrix} \mathbf{D}_1 & 0 \\ \mathbf{D}_3 & \mathbf{D}_2 \end{bmatrix} \begin{bmatrix} \mathbf{R}_1^\top \\ \mathbf{R}_2^\top \end{bmatrix} := \bar{\mathbf{U}}_k \bar{\mathbf{D}}_k \bar{\mathbf{R}}_k^\top,$$

where $\mathbf{D}_1 \in \mathbb{R}^{r \times r}$, $\mathbf{D}_2 \in \mathbb{R}^{r_k \times r_k}$ are not necessarily diagonal matrices, and $\bar{\mathbf{R}}_k$ is orthogonal matrix. Then we have $\Gamma_k = \begin{bmatrix} \mathbf{V}_k^\top \\ \mathbf{W}_k^\top \end{bmatrix} \begin{bmatrix} \mathbf{V}_k & \mathbf{W}_k \end{bmatrix} = \bar{\mathbf{D}}_k \bar{\mathbf{D}}_k^\top$. We denote $\Xi_k = \mathbf{A}_k^* \mathbf{E}_k^\top + \mathbf{E}_k \mathbf{A}_k^{*\top} + \mathbf{E}_k \mathbf{E}_k^\top - d_k \sigma_k^2 \mathbf{I}$. Then from (12), we have $\text{SNR}_k^2 \gtrsim \kappa_k^2 n + \sqrt{nd_k}$, which implies $\|\Xi_k\| \lesssim \lambda_{k,\min}^2$. Then from (Xia, 2021, Theorem 1), we can expand $\Delta_k = \tilde{\mathbf{U}}_k \tilde{\mathbf{U}}_k^\top - \bar{\mathbf{U}}_k \bar{\mathbf{U}}_k^\top$ as follows:

$$\begin{aligned} & \tilde{\mathbf{U}}_k \tilde{\mathbf{U}}_k^\top - \bar{\mathbf{U}}_k \bar{\mathbf{U}}_k^\top \\ &= \sum_{l \geq 1} \sum_{\mathbf{s} \in \mathcal{S}_l} \underbrace{(-1)^{\|\mathbf{s}\|_0 + 1} \mathbf{N}_k(s_1) \Gamma_k^{-s_1} \mathbf{N}_k(s_1)^\top \Xi_k \mathbf{N}_k(s_2) \cdots \mathbf{N}_k(s_l)^\top \Xi_k \mathbf{N}_k(s_{l+1}) \Gamma_k^{-s_{l+1}} \mathbf{N}_k(s_{l+1})^\top}_{:=\mathbf{S}_{k,l}(\mathbf{s})}, \end{aligned} \tag{19}$$

where $\Gamma_k^{-s} = (\bar{\mathbf{D}}_k \bar{\mathbf{D}}_k^\top)^{-s}$ for $s > 0$ and $\Gamma_k^{-0} = \mathbf{I}_{\bar{r}_k}$, and $\mathbf{N}_k(0) = \bar{\mathbf{U}}_{k\perp}$, $\mathbf{N}_k(s) = \bar{\mathbf{U}}_k$ for $s > 0$.

Then the following matrices can be written in terms of $\mathbf{G}_k, \mathbf{H}_k$:

$$\bar{\mathbf{U}}_k^\top \boldsymbol{\Xi}_k \bar{\mathbf{U}}_k = \bar{\mathbf{D}}_k \bar{\mathbf{R}}_k^\top \mathbf{G}_k^\top + \mathbf{G}_k \bar{\mathbf{R}}_k \bar{\mathbf{D}}_k^\top + \mathbf{G}_k \mathbf{G}_k^\top - d_k \sigma_k^2 \mathbf{I}, \quad (20a)$$

$$\bar{\mathbf{U}}_k^\top \boldsymbol{\Xi}_k \bar{\mathbf{U}}_{k\perp} = \bar{\mathbf{D}}_k \bar{\mathbf{R}}_k^\top \mathbf{H}_k^\top + \mathbf{G}_k \mathbf{H}_k^\top, \quad (20b)$$

$$\bar{\mathbf{U}}_{k\perp}^\top \boldsymbol{\Xi}_k \bar{\mathbf{U}}_{k\perp} = \mathbf{H}_k \mathbf{H}_k^\top - d_k \sigma_k^2 \mathbf{I}. \quad (20c)$$

We begin with the upper bounds for $\left\| (\boldsymbol{\Gamma}_k)^{-\frac{1}{2}} \bar{\mathbf{U}}_k^\top \boldsymbol{\Xi}_k \bar{\mathbf{U}}_k (\boldsymbol{\Gamma}_k)^{-\frac{1}{2}} \right\|$, $\left\| \bar{\mathbf{U}}_{k\perp}^\top \boldsymbol{\Xi}_k \bar{\mathbf{U}}_k (\boldsymbol{\Gamma}_k)^{-\frac{1}{2}} \right\|$, and $\left\| \bar{\mathbf{U}}_{k\perp}^\top \boldsymbol{\Xi}_k \bar{\mathbf{U}}_{k\perp} \right\|$. We have

$$(\boldsymbol{\Gamma}_k)^{-\frac{1}{2}} \bar{\mathbf{U}}_k^\top \boldsymbol{\Xi}_k \bar{\mathbf{U}}_k (\boldsymbol{\Gamma}_k)^{-\frac{1}{2}} = (\bar{\mathbf{D}}_k \bar{\mathbf{D}}_k^\top)^{-\frac{1}{2}} (\bar{\mathbf{D}}_k \bar{\mathbf{R}}_k^\top \mathbf{G}_k^\top + \mathbf{G}_k \bar{\mathbf{R}}_k \bar{\mathbf{D}}_k^\top + \mathbf{G}_k \mathbf{G}_k^\top - d_k \sigma_k^2 \mathbf{I}) (\bar{\mathbf{D}}_k \bar{\mathbf{D}}_k^\top)^{-\frac{1}{2}},$$

and thus under \mathcal{E}_k it is bounded by

$$\left\| (\boldsymbol{\Gamma}_k)^{-\frac{1}{2}} \bar{\mathbf{U}}_k^\top \boldsymbol{\Xi}_k \bar{\mathbf{U}}_k (\boldsymbol{\Gamma}_k)^{-\frac{1}{2}} \right\| \lesssim (\bar{r}_k + \delta_k)^{1/2} \lambda_{k,\min}^{-1} (\sigma_k + d_k^{1/2} \lambda_{k,\min}^{-1} \sigma_k^2).$$

And

$$(\boldsymbol{\Gamma}_k)^{-\frac{1}{2}} \bar{\mathbf{U}}_k^\top \boldsymbol{\Xi}_k \bar{\mathbf{U}}_{k\perp} = (\bar{\mathbf{D}}_k \bar{\mathbf{D}}_k^\top)^{-\frac{1}{2}} (\bar{\mathbf{D}}_k \bar{\mathbf{R}}_k^\top \mathbf{H}_k^\top + \mathbf{G}_k \mathbf{H}_k^\top),$$

which is bounded by

$$\left\| (\boldsymbol{\Gamma}_k)^{-\frac{1}{2}} \bar{\mathbf{U}}_k^\top \boldsymbol{\Xi}_k \bar{\mathbf{U}}_{k\perp} \right\| \lesssim n^{1/2} \sigma_k + (nd_k)^{1/2} \lambda_{k,\min}^{-1} \sigma_k^2.$$

under \mathcal{E}_k . And

$$\bar{\mathbf{U}}_{k\perp}^\top \boldsymbol{\Xi}_k \bar{\mathbf{U}}_{k\perp} = \mathbf{H}_k \mathbf{H}_k^\top - d_k \sigma_k^2 \mathbf{I},$$

which is bounded by

$$\left\| \bar{\mathbf{U}}_{k\perp}^\top \boldsymbol{\Xi}_k \bar{\mathbf{U}}_{k\perp} \right\| \lesssim ((n \vee d_k) n)^{1/2} \sigma_k^2.$$

under \mathcal{E}_k . So we conclude if we choose $\delta_k = n \wedge d_k$,

$$\begin{aligned} & \max \left\{ \left\| (\boldsymbol{\Gamma}_k)^{-\frac{1}{2}} \bar{\mathbf{U}}_k^\top \boldsymbol{\Xi}_k \bar{\mathbf{U}}_k (\boldsymbol{\Gamma}_k)^{-\frac{1}{2}} \right\|, \lambda_{k,\min}^{-1} \left\| (\boldsymbol{\Gamma}_k)^{-\frac{1}{2}} \bar{\mathbf{U}}_k^\top \boldsymbol{\Xi}_k \bar{\mathbf{U}}_{k\perp} \right\|, \lambda_{k,\min}^{-2} \left\| \bar{\mathbf{U}}_{k\perp}^\top \boldsymbol{\Xi}_k \bar{\mathbf{U}}_{k\perp} \right\| \right\} \\ & \lesssim n^{1/2} \lambda_{k,\min}^{-1} \sigma_k + (nd_k)^{1/2} \lambda_{k,\min}^{-2} \sigma_k^2 = \varepsilon_k \end{aligned} \quad (21)$$

under the signal to noise ratio: $\lambda_{k,\min}/\sigma_k \gtrsim n^{1/2} \vee (nd_k)^{1/4}$.

We summarize some important observations about $\boldsymbol{\Delta}_k$ in the following lemmas. The first is an immediate consequence of (21) and the expansion of $\boldsymbol{\Delta}_k$ in (19).

Lemma 4. We have $\|\Delta_k\| \cdot 1(\mathcal{E}_k) \leq C\varepsilon_k$.

And the proof of the following lemma is given in section C.4.

Lemma 5. The expectation of $\bar{U}_k^\top \Delta_k \bar{U}_{k\perp} \cdot 1(\mathcal{E}_k)$ is zero, i.e., $\mathbb{E} \bar{U}_k^\top \Delta_k \bar{U}_{k\perp} \cdot 1(\mathcal{E}_k) = 0$.

Now we are ready to prove the lemma. The proof of the lemmas involved can be found in the appendix.

Bounding $\left\| \sum_{k=1}^K w_k \mathbf{U}^\top \Delta_k \mathbf{U}_\perp \Lambda^{-1} \cdot 1(\mathcal{E}_k) \right\|$. Since $\mathbf{U}^\top \bar{U}_{k\perp} = 0$, we have the following decomposition:

$$\begin{aligned} & \sum_{k=1}^K w_k \mathbf{U}^\top \Delta_k \mathbf{U}_\perp \Lambda^{-1} \cdot 1(\mathcal{E}_k) \\ = & \sum_{k=1}^K w_k \underbrace{\mathbf{U}^\top \bar{U}_k \bar{U}_k^\top \Delta_k \bar{U}_k \bar{U}_k^\top \mathbf{U}_\perp \Lambda^{-1}}_{:=\mathbf{R}_k} \cdot 1(\mathcal{E}_k) + \sum_{k=1}^K w_k \underbrace{\mathbf{U}^\top \bar{U}_k \bar{U}_k^\top \Delta_k \bar{U}_{k\perp} \bar{U}_{k\perp}^\top \mathbf{U}_\perp \Lambda^{-1}}_{:=\mathbf{Q}_k} \cdot 1(\mathcal{E}_k). \end{aligned}$$

First the following lemma provides the gives the expectation of $\mathbb{E} \mathbf{R}_k \cdot 1(\mathcal{E}_k)$.

Lemma 6. We have for all $k \in [K]$,

$$\mathbb{E} \mathbf{R}_k \cdot 1(\mathcal{E}_k) = \sum_{r \geq 1} c_{k,r} \mathbf{U}^\top \bar{U}_k \Gamma_k^{-r} \bar{U}_k^\top \mathbf{U}_\perp \Lambda^{-1},$$

where $c_{k,r}$ satisfies $\sum_{r \geq 1} c_{k,r} \lambda_{k,\min}^{-2r} \leq C\varepsilon_k^2$.

Next the following lemma controls the upper bound for

$$\left\| \sum_{k=1}^K w_k \mathbf{R}_k \cdot 1(\mathcal{E}_k) - \mathbb{E} \sum_{k=1}^K w_k \mathbf{R}_k \cdot 1(\mathcal{E}_k) \right\|.$$

Lemma 7. We have

$$\mathbb{P} \left(\left\| \sum_{k=1}^K w_k \mathbf{R}_k \cdot 1(\mathcal{E}_k) - \mathbb{E} \sum_{k=1}^K w_k \mathbf{R}_k \cdot 1(\mathcal{E}_k) \right\| \geq C \sqrt{\sum_{k=1}^K w_k^2 \varepsilon_k^4 \theta^{-2} \sqrt{\log n}} \right) \leq n^{-10}.$$

Finally, we consider the upper bound for $\left\| \sum_{k=1}^K w_k \mathbf{Q}_k \cdot 1(\mathcal{E}_k) \right\|$.

Lemma 8. *We have*

$$\mathbb{P}\left(\left\|\sum_{k=1}^K w_k \mathbf{Q}_k \cdot 1(\mathcal{E}_k)\right\| \geq C \sqrt{\sum_{k=1}^K n^{-1} w_k^2 (\text{tr}(\mathbf{M}_k) + \bar{r}_k \|\mathbf{M}_k\|) \varepsilon_k^2 \sqrt{\log(n)}}\right) \leq n^{-10},$$

where $\mathbf{M}_k = \bar{\mathbf{U}}_{k\perp}^\top \mathbf{U}_\perp \mathbf{\Lambda}^{-2} \mathbf{U}_\perp^\top \bar{\mathbf{U}}_{k\perp}$.

Combining these lemmas and we get the desired bound for $\left\|\sum_{k=1}^K w_k \mathbf{U}^\top \mathbf{\Delta}_k \mathbf{U}_\perp \mathbf{\Lambda}^{-1} \cdot 1(\mathcal{E}_k)\right\|$.

Bounding $\left\|\sum_{k=1}^K w_k \mathbf{U}^\top \mathbf{\Delta}_k \mathbf{U} \cdot 1(\mathcal{E}_k)\right\|$. We have

$$\left\|\sum_{k=1}^K w_k \mathbf{U}^\top \mathbf{\Delta}_k \mathbf{U} \cdot 1(\mathcal{E}_k)\right\| = \left\|\sum_{k=1}^K w_k \mathbf{U}^\top \bar{\mathbf{U}}_k \cdot \underline{\bar{\mathbf{U}}_k^\top \mathbf{\Delta}_k \bar{\mathbf{U}}_k} \cdot \bar{\mathbf{U}}_k^\top \mathbf{U} \cdot 1(\mathcal{E}_k)\right\| \leq \sum_{k=1}^K w_k \varepsilon_k^2.$$

Bounding $\left\|\sum_{k=1}^K w_k \mathbf{U}_\perp^\top \mathbf{\Delta}_k \mathbf{U}_\perp \cdot 1(\mathcal{E}_k)\right\|$. It can be written as

$$\begin{aligned} & \left\|\sum_{k=1}^K w_k \mathbf{U}_\perp^\top \mathbf{\Delta}_k \mathbf{U}_\perp \cdot 1(\mathcal{E}_k)\right\| \\ & \leq \left\|\sum_{k=1}^K w_k \mathbf{U}_\perp^\top \bar{\mathbf{U}}_k \underline{\bar{\mathbf{U}}_k^\top \mathbf{\Delta}_k \bar{\mathbf{U}}_k} \bar{\mathbf{U}}_k^\top \mathbf{U}_\perp \cdot 1(\mathcal{E}_k)\right\| + \left\|\sum_{k=1}^K w_k \mathbf{U}_\perp^\top \bar{\mathbf{U}}_{k\perp} \underline{\bar{\mathbf{U}}_{k\perp}^\top \mathbf{\Delta}_k \bar{\mathbf{U}}_{k\perp}} \bar{\mathbf{U}}_{k\perp}^\top \mathbf{U}_\perp \cdot 1(\mathcal{E}_k)\right\| \\ & \quad + \left\|\sum_{k=1}^K w_k \mathbf{U}_\perp^\top \bar{\mathbf{U}}_{k\perp} \underline{\bar{\mathbf{U}}_{k\perp}^\top \mathbf{\Delta}_k \bar{\mathbf{U}}_k} \bar{\mathbf{U}}_k^\top \mathbf{U}_\perp \cdot 1(\mathcal{E}_k)\right\| + \left\|\sum_{k=1}^K w_k \mathbf{U}_\perp^\top \bar{\mathbf{U}}_{k\perp} \underline{\bar{\mathbf{U}}_{k\perp}^\top \mathbf{\Delta}_k \bar{\mathbf{U}}_k} \bar{\mathbf{U}}_k^\top \mathbf{U}_\perp \cdot 1(\mathcal{E}_k)\right\|. \end{aligned}$$

For the first two terms on the right hand side, we have

$$\begin{aligned} & \left\|\sum_{k=1}^K w_k \mathbf{U}_\perp^\top \bar{\mathbf{U}}_k \underline{\bar{\mathbf{U}}_k^\top \mathbf{\Delta}_k \bar{\mathbf{U}}_k} \bar{\mathbf{U}}_k^\top \mathbf{U}_\perp \cdot 1(\mathcal{E}_k)\right\| \leq C \sum_{k=1}^K w_k \varepsilon_k^2, \\ & \left\|\sum_{k=1}^K w_k \mathbf{U}_\perp^\top \bar{\mathbf{U}}_{k\perp} \underline{\bar{\mathbf{U}}_{k\perp}^\top \mathbf{\Delta}_k \bar{\mathbf{U}}_{k\perp}} \bar{\mathbf{U}}_{k\perp}^\top \mathbf{U}_\perp \cdot 1(\mathcal{E}_k)\right\| \leq C \sum_{k=1}^K w_k \varepsilon_k^2. \end{aligned}$$

For the last two terms, we can use Lemma 9 and we have with probability exceeding $1 - 2n^{-10}$,

$$\begin{aligned} & \left\|\sum_{k=1}^K w_k \mathbf{U}_\perp^\top \bar{\mathbf{U}}_{k\perp} \underline{\bar{\mathbf{U}}_{k\perp}^\top \mathbf{\Delta}_k \bar{\mathbf{U}}_k} \bar{\mathbf{U}}_k^\top \mathbf{U}_\perp \cdot 1(\mathcal{E}_k)\right\| \leq C \sqrt{\sum_{k=1}^K w_k^2 \varepsilon_k^2 \sqrt{\log(n)}}, \\ & \left\|\sum_{k=1}^K w_k \mathbf{U}_\perp^\top \bar{\mathbf{U}}_k \underline{\bar{\mathbf{U}}_k^\top \mathbf{\Delta}_k \bar{\mathbf{U}}_{k\perp}} \bar{\mathbf{U}}_{k\perp}^\top \mathbf{U}_\perp \cdot 1(\mathcal{E}_k)\right\| \leq C \sqrt{\sum_{k=1}^K w_k^2 \varepsilon_k^2 \sqrt{\log(n)}}. \end{aligned}$$

In conclusion, we have

$$\left\| \sum_{k=1}^K w_k \mathbf{U}_\perp^\top \Delta_k \mathbf{U}_\perp \cdot 1(\mathcal{E}_k) \right\| \leq C \sum_{k=1}^K w_k \varepsilon_k^2 + C \sqrt{\sum_{k=1}^K w_k^2 \varepsilon_k^2} \sqrt{\log(n)}.$$

Finally, notice that the upper bound for $\left\| \sum_{k=1}^K w_k \mathbf{U}^\top \Delta_k \mathbf{U}_\perp \cdot 1(\mathcal{E}_k) \right\|$ can be proved using Lemma 6 - Lemma 8 with $\mathbf{\Lambda} = \mathbf{I}$. In fact, from the lemmas above, we conclude

$$\left\| \sum_{k=1}^K w_k \mathbf{U}^\top \Delta_k \mathbf{U}_\perp \cdot 1(\mathcal{E}_k) \right\| \leq C \sqrt{\sum_{k=1}^K w_k^2 \varepsilon_k^2} \sqrt{\log n} + \left\| \sum_{k=1}^K w_k \sum_{r \geq 1} c_{k,r} \mathbf{U}^\top \bar{\mathbf{U}}_k \mathbf{\Gamma}_k^{-r} \bar{\mathbf{U}}_k^\top \mathbf{U}_\perp \right\|.$$

Notice that

$$\left\| \sum_{r \geq 1} c_{k,r} \mathbf{U}^\top \bar{\mathbf{U}}_k \mathbf{\Gamma}_k^{-r} \bar{\mathbf{U}}_k^\top \mathbf{U}_\perp \right\| \leq \sum_{r \geq 1} |c_{k,r}| \lambda_{k,\min}^{-2r} \leq C \varepsilon_k^2$$

and we finish the proof.

C.2 Proof of Lemma 2

We first show that for any $\mathbf{w}, \mathbf{w}' \in \Delta_K$,

$$|\theta(\mathbf{w}) - \theta(\mathbf{w}')| \leq \|\mathbf{w} - \mathbf{w}'\|_1. \quad (22)$$

Denote $\mathbf{B}(\mathbf{w}) := \sum_{k=1}^K w_k \mathbf{U}_k \mathbf{U}_k^\top$, then $\theta(\mathbf{w}) = 1 - \lambda_{\max}(\mathbf{B}(\mathbf{w}))$. Notice that

$$\|\mathbf{B}(\mathbf{w}) - \mathbf{B}(\mathbf{w}')\| \leq \sum_{k=1}^K |w_k - w'_k| = \|\mathbf{w} - \mathbf{w}'\|_1.$$

By Weyl's inequality, we thus get

$$|\theta(\mathbf{w}) - \theta(\mathbf{w}')| = |\lambda_{\max}(\mathbf{B}(\mathbf{w})) - \lambda_{\max}(\mathbf{B}(\mathbf{w}'))| \leq \|\mathbf{B}(\mathbf{w}) - \mathbf{B}(\mathbf{w}')\| \leq \|\mathbf{w} - \mathbf{w}'\|_1.$$

Then for any $\mathbf{w} \in \Omega_{\theta_0}(\mathbf{w}^\dagger)$,

$$\theta(\mathbf{w}) \geq \theta(\mathbf{w}^\dagger) - \|\mathbf{w} - \mathbf{w}^\dagger\| \geq \theta_0 > 0.$$

Next, we show that for any $\mathbf{w}, \mathbf{w}' \in \Omega_{\theta_0}(\mathbf{w}^\dagger)$,

$$\|\mathbf{M}_k(\mathbf{w}) - \mathbf{M}_k(\mathbf{w}')\| \leq 2\theta_0^{-3} \|\mathbf{w} - \mathbf{w}'\|_1, \quad \forall k \in [K]. \quad (23)$$

Let $\mathbf{H}(\mathbf{w}) := \mathbf{I} - \mathbf{U}\mathbf{U}^\top - \mathbf{B}(\mathbf{w})$. Then we have

$$\|\mathbf{H}(\mathbf{w}) - \mathbf{H}(\mathbf{w}')\| \leq \|\mathbf{w} - \mathbf{w}'\|_1.$$

On the orthogonal complement of $\text{span}\{\mathbf{U}, \{\mathbf{U}_k\}\}$, the eigenvalues of $\mathbf{H}(\mathbf{w})$ are those of $\mathbf{A}(\mathbf{w})$ and lie in $[\theta_0, 1]$. Consider $f(x) = x^{-2}$ on $[\theta_0, 1]$ and the matrix function $f(\mathbf{H}(\mathbf{w}))$, then

$$Df(\mathbf{H})[\Delta] = -\mathbf{H}^{-1}\Delta\mathbf{H}^{-2} - \mathbf{H}^{-2}\Delta\mathbf{H}^{-1}.$$

Using $\|\mathbf{H}^{-1}\| \leq \theta_0^{-1}$, we thus arrive at $\|Df(\mathbf{H})[\Delta]\| \leq 2\theta_0^{-3}\|\Delta\|$. It follows that

$$\|f(\mathbf{H}(\mathbf{w})) - f(\mathbf{H}(\mathbf{w}'))\| \leq 2\theta_0^{-3}\|\mathbf{H}(\mathbf{w}) - \mathbf{H}(\mathbf{w}')\| \leq 2\theta_0^{-3}\|\mathbf{w} - \mathbf{w}'\|_1.$$

Therefore, we get

$$\|\mathbf{M}_k(\mathbf{w}) - \mathbf{M}_k(\mathbf{w}')\| \leq \|f(\mathbf{H}(\mathbf{w})) - f(\mathbf{H}(\mathbf{w}'))\| \leq 2\theta_0^{-3}\|\mathbf{w} - \mathbf{w}'\|_1.$$

Equipped with (22) and (23), we can prove our desired result. By definition, we get

$$\begin{aligned} |c_k(\mathbf{w}) - c_k(\mathbf{w}')| &\leq \varepsilon_k^4 |\theta(\mathbf{w})^{-2} - \theta(\mathbf{w}')^{-2}| \\ &\quad + n^{-1} \varepsilon_k^2 \left(|\text{tr}\mathbf{M}_k(\mathbf{w}) - \text{tr}\mathbf{M}_k(\mathbf{w}')| + \bar{r}_k \left| \|\mathbf{M}_k(\mathbf{w})\| - \|\mathbf{M}_k(\mathbf{w}')\| \right| \right). \end{aligned}$$

The proof is completed by using (22), (23), $|x^{-2} - y^{-2}| \leq 2\theta_0^{-3}|x - y|$ for $x, y \geq \theta_0$, and

$$|\text{tr}\mathbf{M}_k(\mathbf{w}) - \text{tr}\mathbf{M}_k(\mathbf{w}')| \leq 2\bar{r}_k \|\mathbf{M}_k(\mathbf{w}) - \mathbf{M}_k(\mathbf{w}')\| \leq 4\bar{r}_k \theta_0^{-3} \|\mathbf{w} - \mathbf{w}'\|_1.$$

C.3 Proof of Lemma 3

Denote $\mathbf{B}(\mathbf{w}) := \sum_{k=1}^K w_k \mathbf{U}_k \mathbf{U}_k^\top$. The map $w \mapsto \mathbf{B}(\mathbf{w})$ is affine in \mathbf{w} and hence C^1 . Since each positive eigenvalue of $\mathbf{B}(\mathbf{w}^\dagger)$ is simple, by Theorem 6.8 in Kato (2013) we can claim that there exists a neighborhood Ω of \mathbf{w}^\dagger and C^1 maps $\mathbf{w} \mapsto \lambda_i(\mathbf{w})$ and $\mathbf{w} \mapsto \mathbf{v}_i(\mathbf{w})$ for each positive eigenpair $(\lambda_i^\dagger, \mathbf{v}_i^\dagger)$ of $\mathbf{B}(\mathbf{w}^\dagger)$. In particular, the top eigenpair $(\lambda_{\max}(\mathbf{B}(\mathbf{w})), \mathbf{v}_{\max}(\mathbf{w}))$ is C^1 on Ω , which implies $\theta(\mathbf{w}) = 1 - \lambda_{\max}(\mathbf{B}(\mathbf{w}))$ is also C^1 .

Define $\mathbf{H}(\mathbf{w}) := \mathbf{I} - \mathbf{U}\mathbf{U}^\top - \mathbf{B}(\mathbf{w})$. Notice that

$$\mathbf{H}(\mathbf{w})\mathbf{x} = (\mathbf{I} - \mathbf{B}(\mathbf{w}))\mathbf{x}, \quad \mathbf{x} \in \text{span}(\mathbf{U}_\perp),$$

so the positive eigenvalues of $\mathbf{H}(\mathbf{w})$ are exactly $1 - \lambda_i(\mathbf{w})$ with eigenvectors $\mathbf{v}_i(\mathbf{w})$. Thus the same perturbation results applied to $\mathbf{B}(\mathbf{w})$ yield C^1 dependence of the positive eigenpairs of $\mathbf{H}(\mathbf{w})$, and hence C^1 maps $\mathbf{w} \mapsto \mathbf{\Lambda}(\mathbf{w})$ and $\mathbf{w} \mapsto \mathbf{U}_\perp(\mathbf{w})$. Since all positive eigenvalues in $\mathbf{\Lambda}(\mathbf{w})$ lie in $[\theta_0, 1]$, hence the map $\mathbf{w} \mapsto \mathbf{\Lambda}(\mathbf{w})^{-2}$ is C^1 . We thus arrive at

$$\mathbf{M}_k(\mathbf{w}) = \bar{\mathbf{U}}_{k\perp}^\top \mathbf{U}_\perp(\mathbf{w}) \mathbf{\Lambda}(\mathbf{w})^{-2} \mathbf{U}_\perp(\mathbf{w})^\top \bar{\mathbf{U}}_{k\perp}$$

is also C^1 in \mathbf{w} on Ω for each $k \in [K]$. The definitions of $c_k(\mathbf{w})$ and $J(\mathbf{w}) = \sum_{k=1}^K w_k^2 c_k(\mathbf{w})$ then show that they are also C^1 on Ω .

C.4 Proof of Lemma 5

We will prove this by showing the expectation $\mathbb{E} \bar{\mathbf{U}}_k^\top \mathbf{S}_{k,l}(\mathbf{s}) \bar{\mathbf{U}}_{k\perp} \cdot 1(\mathcal{E}_k)$ is zero. Notice $\bar{\mathbf{U}}_k^\top \mathbf{S}_{k,l}(\mathbf{s}) \bar{\mathbf{U}}_{k\perp}$ is also equal to

$$\bar{\mathbf{U}}_k^\top \mathbf{N}_k(s_1) \mathbf{\Gamma}_k^{-s_1} \mathbf{N}_k(s_1)^\top \underline{\mathbf{\Xi}_k \mathbf{N}_k(s_2)} \cdots \underline{\mathbf{N}_k(s_l)^\top \mathbf{\Xi}_k \mathbf{N}_k(s_{l+1})} \mathbf{\Gamma}_k^{-s_{l+1}} \mathbf{N}_k(s_{l+1})^\top \bar{\mathbf{U}}_{k\perp} \cdot 1(\mathcal{E}_k). \quad (24)$$

For (24) to be non-zero, we have $s_1 > 0, s_{l+1} = 0$. Recall the notation in (20):

$$\begin{aligned} \bar{\mathbf{U}}_k^\top \mathbf{\Xi}_k \bar{\mathbf{U}}_k &= \bar{\mathbf{D}}_k \bar{\mathbf{R}}_k^\top \mathbf{G}_k^\top + \mathbf{G}_k \bar{\mathbf{R}}_k \bar{\mathbf{D}}_k^\top + \mathbf{G}_k \mathbf{G}_k^\top - d_k \sigma_k^2 \mathbf{I}, \\ \bar{\mathbf{U}}_k^\top \mathbf{\Xi}_k \bar{\mathbf{U}}_{k\perp} &= \bar{\mathbf{D}}_k \bar{\mathbf{R}}_k^\top \mathbf{H}_k^\top + \mathbf{G}_k \mathbf{H}_k^\top, \\ \bar{\mathbf{U}}_{k\perp}^\top \mathbf{\Xi}_k \bar{\mathbf{U}}_{k\perp} &= \mathbf{H}_k \mathbf{H}_k^\top - d_k \sigma_k^2 \mathbf{I}. \end{aligned}$$

We define $\mathbf{C}_1 := \bar{\mathbf{U}}_k^\top \mathbf{\Xi}_k \bar{\mathbf{U}}_k$. When $t \geq 2$, we define

$$\mathbf{C}_t := \mathbf{\Gamma}_k^{-1/2} \bar{\mathbf{U}}_k^\top \mathbf{\Xi}_k \bar{\mathbf{U}}_{k\perp} \cdot \underbrace{\bar{\mathbf{U}}_{k\perp}^\top \mathbf{\Xi}_k \bar{\mathbf{U}}_{k\perp} \cdots \bar{\mathbf{U}}_{k\perp}^\top \mathbf{\Xi}_k \bar{\mathbf{U}}_{k\perp}}_{t-2 \text{ of } \bar{\mathbf{U}}_{k\perp}^\top \mathbf{\Xi}_k \bar{\mathbf{U}}_{k\perp}} \cdot \bar{\mathbf{U}}_{k\perp}^\top \mathbf{\Xi}_k \bar{\mathbf{U}}_k \mathbf{\Gamma}_k^{-1/2}. \quad (25)$$

Then (24) can be written as

$$\mathbf{\Gamma}_k^{-a_0+1/2} \cdot \mathbf{C}_{t_1} \cdot \mathbf{\Gamma}_k^{-a_1+1} \cdots \mathbf{\Gamma}_k^{-a_{p-1}+1} \cdot \mathbf{C}_{t_p} \cdot \mathbf{\Gamma}_k^{-a_p+1/2} \cdot \bar{\mathbf{U}}_k^\top \mathbf{\Xi}_k \bar{\mathbf{U}}_{k\perp} \cdot (\bar{\mathbf{U}}_{k\perp}^\top \mathbf{\Xi}_k \bar{\mathbf{U}}_{k\perp})^{t_{p+1}} \cdot 1(\mathcal{E}_k), \quad (26)$$

where $t_1 + \cdots + t_p + t_{p+1} + 1 = a_0 + \cdots + a_p = l$. If we condition on \mathbf{G}_k , then we can view \mathbf{C}_t as a function of \mathbf{H}_k , and $\mathbf{C}_t(\mathbf{H}_k) = \mathbf{C}_t(-\mathbf{H}_k)$, $\bar{\mathbf{U}}_{k\perp}^\top \mathbf{\Xi}_k \bar{\mathbf{U}}_{k\perp}$ is also even in \mathbf{H}_k . And $\bar{\mathbf{U}}_k^\top \mathbf{\Xi}_k \bar{\mathbf{U}}_{k\perp}$ is odd in \mathbf{H}_k . Moreover, $1(\mathcal{E}_k)$ is even in \mathbf{H}_k . So we can conclude (26) is a odd function in \mathbf{H}_k , and thus it has mean-zero.

C.5 Proof of Lemma 6

Recall the expansion of Δ_k in (19). In order for $\bar{U}_k^\top \mathbf{S}_{k,l}(\mathbf{s}) \bar{U}_k$ to be non-zero, $s_1, s_{l+1} > 0$ (since $\bar{U}_k^\top \bar{U}_{k\perp} = 0$). This also indicates $\bar{U}_k^\top \mathbf{S}_{k,1}(\mathbf{s}) \bar{U}_k = 0$. For each $l \geq 2$, $\mathbf{s} \in \mathbb{S}_l$, we consider the expectation of

$$\mathbb{E} \mathbf{U}^\top \bar{U}_k \Gamma_k^{-s_1} \bar{U}_k^\top \underline{\Xi}_k \mathbf{N}_k(s_2) \cdots \mathbf{N}_k(s_l)^\top \underline{\Xi}_k \bar{U}_k \Gamma_k^{-s_{l+1}} \bar{U}_k^\top \mathbf{U}_\perp \cdot 1(\mathcal{E}_k).$$

We will first focus on the expectation:

$$\mathbb{E} \Gamma_k^{-s_1} \bar{U}_k^\top \underline{\Xi}_k \mathbf{N}_k(s_2) \cdots \mathbf{N}_k(s_l)^\top \underline{\Xi}_k \bar{U}_k \Gamma_k^{-s_{l+1}} \cdot 1(\mathcal{E}_k).$$

Recall the definition of \mathbf{C}_t in (25), and we have

$$\begin{aligned} \mathbf{C}_1 &= \mathbf{G}_{k1}^\top \Gamma_k^{-1/2} + \Gamma_k^{-1/2} \mathbf{G}_{k1} + \Gamma_k^{-1/2} \mathbf{G}_{k1} \mathbf{G}_{k1}^\top \Gamma_k^{-1/2} + \Gamma_k^{-1/2} \mathbf{G}_{k2} \mathbf{G}_{k2}^\top \Gamma_k^{-1/2} - d_k \sigma_k^2 \Gamma_k^{-1} \\ \mathbf{C}_t &= (\mathbf{H}_{k1}^\top + \Gamma_k^{-1/2} \mathbf{G}_{k1} \mathbf{H}_{k1}^\top + \Gamma_k^{-1/2} \mathbf{G}_{k2} \mathbf{H}_{k2}^\top) (\mathbf{H}_k \mathbf{H}_k^\top - d_k \sigma_k^2 \mathbf{I})^{t-2} \\ &\quad (\mathbf{H}_{k1} + \mathbf{H}_{k1} \mathbf{G}_{k1}^\top \Gamma_k^{-1/2} + \mathbf{H}_{k2} \mathbf{G}_{k2}^\top \Gamma_k^{-1/2}), \end{aligned}$$

where $\begin{bmatrix} \mathbf{G}_{k1} & \mathbf{G}_{k2} \\ \mathbf{H}_{k1} & \mathbf{H}_{k2} \end{bmatrix} = \begin{bmatrix} \mathbf{G}_k \\ \mathbf{H}_k \end{bmatrix} \begin{bmatrix} \mathbf{Q}_k & \mathbf{Q}_{k\perp} \end{bmatrix}$ for $\mathbf{Q}_k = \bar{\mathbf{R}}_k \bar{\mathbf{D}}_k^\top (\bar{\mathbf{D}}_k \bar{\mathbf{D}}_k^\top)^{-1/2}$. We can also rewrite

$$\begin{aligned} &\mathbb{E} \Gamma_k^{-s_1} \bar{U}_k^\top \underline{\Xi}_k \mathbf{N}_k(s_2) \cdots \mathbf{N}_k(s_l)^\top \underline{\Xi}_k \bar{U}_k \Gamma_k^{-s_{l+1}} \cdot 1(\mathcal{E}_k) \\ &= \mathbb{E} \Gamma_k^{-a_0+1/2} \mathbf{C}_{t_1} \Gamma_k^{-a_1+1} \cdots \mathbf{C}_{t_p} \Gamma_k^{-a_p+1/2} \cdot 1(\mathcal{E}_k) \end{aligned}$$

for some integers $a_0, \dots, a_p, t_1, \dots, t_p > 0$ and $a_0 + \dots + a_p = t_1 + \dots + t_p = l$. Since $\Gamma_k^{-1/2} \mathbf{G}_{k1}$ and $\Gamma_k^{-1/2} \mathbf{G}_{k2}$ has i.i.d. $N(0, \Gamma_k^{-1})$ columns, we can write the expectation as a function of Γ_k^{-1} :

$$\Psi_{l,\mathbf{s}}(\Gamma_k^{-1}) := \mathbb{E} \mathbf{C}_{t_1} \Gamma_k^{-a_1+1} \cdots \mathbf{C}_{t_p} \cdot 1(\mathcal{E}_k).$$

Notice we also have

$$\Psi_{l,\mathbf{s}}(\mathbf{O} \Gamma_k^{-1/2} \mathbf{O}^\top) = \mathbf{O} \Psi_{l,\mathbf{s}}(\Gamma_k^{-1/2}) \mathbf{O}^\top$$

for any orthogonal matrix $\mathbf{O} \in \mathbb{O}_{\bar{r}_k}$. Therefore the function $\Psi_{l,\mathbf{s}}$ is equivariant under the conjugate action of the orthogonal group $\mathbb{O}_{\bar{r}_k}$. From (Procesi, 1976, Theorem 2.1), we have

$$\Psi_{l,\mathbf{s}}(\Gamma_k^{-1}) = \sum_{r=0}^{l-1} c_{l,\mathbf{s},r+1} \Gamma_k^{-r}.$$

for some $c_{l,s,r}$ that depends on Γ_k^{-1} . And thus

$$\mathbb{E}\Gamma_k^{-s_1}\bar{\mathbf{U}}_k^\top\bar{\boldsymbol{\Xi}}_k\mathbf{N}_k(s_2)\cdots\mathbf{N}_k(s_l)^\top\bar{\boldsymbol{\Xi}}_k\bar{\mathbf{U}}_k\Gamma_k^{-s_{l+1}}\cdot\mathbf{1}(\mathcal{E}_k)=\sum_{r=1}^lc_{l,s,r}\Gamma_k^{-r}.$$

Also, under the event \mathcal{E}_k , we can conclude:

$$\sum_{r=1}^l|c_{l,s,r}|\lambda_{k,\min}^{-2r}\leq\varepsilon_k^l.$$

This also implies

$$\mathbb{E}\bar{\mathbf{U}}_k^\top(\tilde{\mathbf{U}}_k\tilde{\mathbf{U}}_k^\top-\bar{\mathbf{U}}_k\bar{\mathbf{U}}_k^\top)\bar{\mathbf{U}}_k\cdot\mathbf{1}(\mathcal{E}_k)=\sum_{r\geq 1}c_{k,r}\Gamma_k^{-r},$$

where $c_{k,r}$ satisfies $\sum_{r\geq 1}c_{k,r}\lambda_{k,\min}^{-2r}\leq C\varepsilon_k^2$. In conclusion, we have

$$\mathbb{E}\mathbf{R}_k\cdot\mathbf{1}(\mathcal{E}_k)=\sum_{r\geq 1}c_{k,r}\mathbf{U}^\top\bar{\mathbf{U}}_k\Gamma_k^{-r}\bar{\mathbf{U}}_k^\top\mathbf{U}\perp\boldsymbol{\Lambda}^{-1}.$$

C.6 Proof of Lemma 7

Recall $\mathbf{R}_k=\mathbf{U}^\top\bar{\mathbf{U}}_k\bar{\mathbf{U}}_k^\top\boldsymbol{\Delta}_k\bar{\mathbf{U}}_k\bar{\mathbf{U}}_k^\top\mathbf{U}\perp\boldsymbol{\Lambda}^{-1}$. Expanding $\boldsymbol{\Delta}_k$ (see (19)) and we have

$$\sum_{k=1}^Kw_k\mathbf{R}_k\cdot\mathbf{1}(\mathcal{E}_k)=\sum_{k=1}^Kw_k\mathbf{U}^\top\bar{\mathbf{U}}_k\underbrace{\sum_{l\geq 2}\sum_{s\in\mathbb{S}_l}\bar{\mathbf{U}}_k^\top\mathbf{S}_{k,l}(s)\bar{\mathbf{U}}_k\bar{\mathbf{U}}_k^\top\mathbf{U}\perp\boldsymbol{\Lambda}^{-1}}_{:=\mathbf{W}_k}\cdot\mathbf{1}(\mathcal{E}_k).$$

Here we use the fact when $l=1$, $\bar{\mathbf{U}}_k^\top\mathbf{S}_{k,1}(s)\bar{\mathbf{U}}_k=0$. And we denote the symmetric version of \mathbf{W}_k as

$$\bar{\mathbf{W}}_k=\begin{bmatrix} 0 & \mathbf{W}_k \\ \mathbf{W}_k^\top & 0 \end{bmatrix}.$$

Then

$$(\bar{\mathbf{W}}_k-\mathbb{E}\bar{\mathbf{W}}_k)^2\leq\begin{bmatrix} \mathbf{W}_k\mathbf{W}_k^\top & 0 \\ 0 & \mathbf{W}_k^\top\mathbf{W}_k \end{bmatrix}\leq\|\mathbf{W}_k^\top\mathbf{W}_k\|\mathbf{I}.$$

Here $\mathbf{A}\leq\mathbf{B}$ means $\mathbf{B}-\mathbf{A}$ is SPSPD. Notice

$$\|\mathbf{W}_k^\top\mathbf{W}_k\|\leq w_k^2\theta^{-2}\sum_{l\geq 2}4^l\varepsilon_k^{2l}\leq Cw_k^2\theta^{-2}\varepsilon_k^4.$$

Now we use matrix Hoeffding for matrices with bounded operator norm, and we have

$$\mathbb{P}\left(\left\|\sum_{k=1}^K(\bar{\mathbf{W}}_k - \mathbb{E}\bar{\mathbf{W}}_k)\right\| \geq C\sqrt{\sum_{k=1}^K w_k^2 \varepsilon_k^4 \theta^{-2} \sqrt{\log n}}\right) \leq n^{-10}.$$

Notice that $\left\|\sum_{k=1}^K w_k \mathbf{R}_k \cdot 1(\mathcal{E}_k) - \mathbb{E}\sum_{k=1}^K w_k \mathbf{R}_k \cdot 1(\mathcal{E}_k)\right\| = \left\|\sum_{k=1}^K(\bar{\mathbf{W}}_k - \mathbb{E}\bar{\mathbf{W}}_k)\right\|$ finalizes the proof.

C.7 Proof of Lemma 8

We state a more general version of Lemma 8.

Lemma 9. *Let $\mathbf{N}_k, \mathbf{O}_k, k \in [K]$ be matrices with $\|\mathbf{O}_k\| \leq 1$. Then for any $p > 0$, with probability exceeding $1 - p$,*

$$\begin{aligned} & \left\|\sum_{k=1}^K \mathbf{O}_k \cdot \bar{\mathbf{U}}_k^\top \Delta_k \bar{\mathbf{U}}_{k\perp} \cdot \mathbf{N}_k \cdot 1(\mathcal{E}_k)\right\| \\ & \leq C\sqrt{\sum_{k=1}^K n^{-1}(\text{tr}(\mathbf{N}_k^\top \mathbf{N}_k) + \bar{r}_k \|\mathbf{N}_k^\top \mathbf{N}_k\|) \varepsilon_k^2 \sqrt{\log(n \vee p^{-1})}}. \end{aligned}$$

Proof. First from Lemma 5, we have $\mathbb{E}\bar{\mathbf{U}}_k^\top \Delta_k \bar{\mathbf{U}}_{k\perp} \cdot 1(\mathcal{E}_k) = 0$. We have

$$\sum_{k=1}^K \mathbf{O}_k \cdot \bar{\mathbf{U}}_k^\top \Delta_k \bar{\mathbf{U}}_{k\perp} \cdot \mathbf{N}_k \cdot 1(\mathcal{E}_k) = \sum_{k=1}^K \mathbf{O}_k \sum_{l \geq 1} \sum_{\mathbf{s} \in \mathbb{S}_l} \bar{\mathbf{U}}_k^\top \mathbf{S}_{k,l}(\mathbf{s}) \bar{\mathbf{U}}_{k\perp} \mathbf{N}_k \cdot 1(\mathcal{E}_k).$$

Now we consider

$$\left\|\sum_{k=1}^K \underbrace{\bar{\mathbf{U}}_k^\top \mathbf{S}_{k,l}(\mathbf{s}) \bar{\mathbf{U}}_{k\perp} \mathbf{N}_k}_{:=\mathbf{W}_k} \cdot 1(\mathcal{E}_k)\right\|$$

for fixed $l \geq 1$ and $\mathbf{s} \in \mathbb{S}_l$. Let $\bar{\mathbf{W}}_k$ be the symmetric version of \mathbf{W}_k :

$$\bar{\mathbf{W}}_k = \begin{bmatrix} 0 & \mathbf{W}_k \\ \mathbf{W}_k^\top & 0 \end{bmatrix}.$$

Then

$$\mathbb{E} \exp(\lambda \bar{\mathbf{W}}_k) = \mathbb{E} \sum_{p \geq 0} \frac{\lambda^p \bar{\mathbf{W}}_k^p}{p!}.$$

Since the odd moments of $\bar{\mathbf{W}}_k$ vanish, we have

$$\mathbb{E} \exp(\lambda \bar{\mathbf{W}}_k) = \mathbb{E} \sum_{p \geq 0} \frac{\lambda^{2p} \bar{\mathbf{W}}_k^{2p}}{(2p)!}.$$

Notice

$$\bar{\mathbf{W}}_k^2 = \begin{bmatrix} \mathbf{W}_k \mathbf{W}_k^\top & 0 \\ 0 & \mathbf{W}_k^\top \mathbf{W}_k \end{bmatrix} \leq \left\| \mathbf{W}_k^\top \mathbf{W}_k \right\| \mathbf{I}.$$

Here $\mathbf{A} \leq \mathbf{B}$ means $\mathbf{B} - \mathbf{A}$ is SPSPD. And therefore

$$\mathbb{E} \bar{\mathbf{W}}_k^{2p} \leq \mathbb{E} \left\| \mathbf{W}_k^\top \mathbf{W}_k \right\|^p \mathbf{I}.$$

Next we bound the ψ_1 norm of $\left\| \mathbf{W}_k^\top \mathbf{W}_k \right\|$. Notice $\bar{\mathbf{U}}_{k\perp}^\top \mathbf{S}_{k,l}(\mathbf{s}) \bar{\mathbf{U}}_k$ must take the form $\mathbf{Z}_k^a \mathbf{Y}_k^\top \mathbf{N}_1$ with

$$\mathbf{Y}_k = (\bar{\mathbf{D}}_k \bar{\mathbf{D}}_k^\top)^{-1/2} (\bar{\mathbf{D}}_k \bar{\mathbf{R}}_k^\top + \mathbf{G}_k) \mathbf{H}_k^\top, \quad \mathbf{Z}_k = \mathbf{H}_k \mathbf{H}_k^\top - d_k \sigma_k^2 \mathbf{I},$$

and $0 \leq a \leq l$, $\|\mathbf{N}_1 \cdot 1(\mathcal{E}_k)\| \leq \varepsilon_k^{l-a-1} \lambda_{k,\min}^{-2a-1}$. Since $\|\mathbf{O}_k\| \leq 1$,

$$\left\| \mathbf{W}_k^\top \mathbf{W}_k \right\| \leq \varepsilon_k^{2l-2a-2} \lambda_{k,\min}^{-4a-2} \left\| \mathbf{Y}_k \mathbf{Z}_k^a \mathbf{N}_k^\top \mathbf{N}_k \mathbf{Z}_k^a \mathbf{Y}_k^\top \right\| \cdot 1(\mathcal{E}_k).$$

Lemma 10. *We have*

$$\lambda_{k,\min}^{-4a-2} \left\| \left\| \mathbf{Y}_k \mathbf{Z}_k^a \mathbf{M}_0 \mathbf{Z}_k^a \mathbf{Y}_k^\top \cdot 1(\mathcal{E}_k) \right\| \right\|_{\psi_1} \leq n^{-1} \varepsilon_k^{2a+2} (\text{tr}(\mathbf{M}_0) + \bar{r}_k \|\mathbf{M}_0\|).$$

for any SPSPD matrix \mathbf{M}_0 .

And thus from Lemma 10,

$$\left\| \left\| \mathbf{W}_k^\top \mathbf{W}_k \right\| \right\|_{\psi_1} \leq n^{-1} \varepsilon_k^{2l} (\text{tr}(\mathbf{N}_k^\top \mathbf{N}_k) + \bar{r}_k \|\mathbf{N}_k^\top \mathbf{N}_k\|).$$

And thus using the moments bound for sub-exponential random variables, we have

$$\mathbb{E} \bar{\mathbf{W}}_k^{2p} \leq \mathbb{E} \left\| \mathbf{W}_k^\top \mathbf{W}_k \right\|^p \mathbf{I} \leq [C n^{-1} \varepsilon_k^{2l} (\text{tr}(\mathbf{N}_k^\top \mathbf{N}_k) + \bar{r}_k \|\mathbf{N}_k^\top \mathbf{N}_k\|)]^p (p!) \mathbf{I}.$$

Therefore

$$\begin{aligned} \mathbb{E} \exp(\lambda \bar{\mathbf{W}}_k) &= \mathbb{E} \sum_{p \geq 0} \frac{\lambda^{2p} \bar{\mathbf{W}}_k^{2p}}{(2p)!} \leq \sum_{p \geq 0} \frac{\lambda^{2p} [C n^{-1} \varepsilon_k^{2l} (\text{tr}(\mathbf{N}_k^\top \mathbf{N}_k) + \bar{r}_k \|\mathbf{N}_k^\top \mathbf{N}_k\|)]^p}{p!} \mathbf{I} \\ &= \exp\left(\frac{1}{2} \lambda^2 \mathbf{V}_k\right), \end{aligned}$$

where $\mathbf{V}_k = Cn^{-1}\varepsilon_k^{2l}(\text{tr}(\mathbf{N}_k^\top \mathbf{N}_k) + \bar{r}_k \|\mathbf{N}_k^\top \mathbf{N}_k\|)\mathbf{I}$. Now from matrix Hoeffding's inequality, we have

$$\mathbb{P}\left(\left\|\sum_{k=1}^K \bar{\mathbf{W}}_k\right\| \geq \sigma_l \sqrt{\log(2n) + \log p_l^{-1}}\right) \leq p_l$$

where $\sigma_l^2 \leq C \sum_{k=1}^K n^{-1}\varepsilon_k^{2l}(\text{tr}(\mathbf{N}_k^\top \mathbf{N}_k) + \bar{r}_k \|\mathbf{N}_k^\top \mathbf{N}_k\|)$ and $p_l > 0$ is to be determined.

Now taking union bound over all $l \geq 1$, and $\mathbf{s} \in \mathbb{S}_l$, we get with probability exceeding $1 - \sum_{l \geq 1} 4^l p_l$,

$$\left\|\sum_{k=1}^K \mathbf{O}_k \bar{\mathbf{U}}_k^\top \Delta_k \bar{\mathbf{U}}_{k\perp} \mathbf{N}_k \cdot 1(\mathcal{E}_k)\right\| \leq \sum_{l \geq 1} 4^l \sigma_l \sqrt{\log(2n) + \log p_l^{-1}}.$$

Now we set $p_l = (4n)^{-l}p$ and we conclude with probability exceeding $1 - p$,

$$\begin{aligned} & \left\|\sum_{k=1}^K \mathbf{O}_k \bar{\mathbf{U}}_k^\top \Delta_k \bar{\mathbf{U}}_{k\perp} \mathbf{N}_k \cdot 1(\mathcal{E}_k)\right\| \\ & \leq \sum_{l \geq 1} C^l \sqrt{\sum_{k=1}^K n^{-1}(\text{tr}(\mathbf{N}_k^\top \mathbf{N}_k) + \bar{r}_k \|\mathbf{N}_k^\top \mathbf{N}_k\|)\varepsilon_k^{2l} \sqrt{\log n + \log p^{-1}}} \\ & \leq \sum_{l \geq 1} \frac{1}{2^l} \sqrt{\sum_{k=1}^K n^{-1}(\text{tr}(\mathbf{N}_k^\top \mathbf{N}_k) + \bar{r}_k \|\mathbf{N}_k^\top \mathbf{N}_k\|)\varepsilon_k^2 \sqrt{\log n + \log p^{-1}}} \\ & \leq 2 \sqrt{\sum_{k=1}^K n^{-1}(\text{tr}(\mathbf{N}_k^\top \mathbf{N}_k) + \bar{r}_k \|\mathbf{N}_k^\top \mathbf{N}_k\|)\varepsilon_k^2 \sqrt{\log n + \log p^{-1}}}, \end{aligned}$$

where we use the fact $\varepsilon_k \leq c_0$ for some small absolute constant. \square

C.8 Proof of Lemma 10

Recall $\mathbf{Y}_k = (\bar{\mathbf{D}}_k \bar{\mathbf{D}}_k^\top)^{-1/2}(\bar{\mathbf{D}}_k \bar{\mathbf{R}}_k^\top + \mathbf{G}_k)\mathbf{H}_k^\top$, and we denote $\mathbf{H}_1 = (\bar{\mathbf{D}}_k \bar{\mathbf{D}}_k^\top)^{-1/2} \bar{\mathbf{D}}_k \mathbf{H}_k^\top$. Then $\mathbf{H}_1 \in \mathbb{R}^{\bar{r}_k \times (n-r)}$ has i.i.d. $N(0, \sigma_k^2)$ entries. Then we have

$$\begin{aligned} & \left\|\mathbf{Y}_k \mathbf{Z}_k^a \mathbf{M}_0 \mathbf{Z}_k^a \mathbf{Y}_k^\top\right\| \cdot 1(\mathcal{E}_k) \\ & \leq 2 \left\|\mathbf{H}_1^\top \mathbf{Z}_k^a \mathbf{M}_0 \mathbf{Z}_k^a \mathbf{H}_1\right\| \cdot 1(\mathcal{E}_k) + 2\lambda_{k,\min}^{-2} \left\|\mathbf{G}_k \mathbf{H}_k^\top \mathbf{Z}_k^a \mathbf{M}_0 \mathbf{Z}_k^a \mathbf{H}_k \mathbf{G}_k^\top\right\| \cdot 1(\mathcal{E}_k) \end{aligned}$$

First we consider $\left\| \left\| \mathbf{G}_k \mathbf{H}_k^\top \mathbf{Z}_k^a \mathbf{M}_0 \mathbf{Z}_k^a \mathbf{H}_k \mathbf{G}_k^\top \right\| \cdot 1(\mathcal{E}_k) \right\|_{\psi_1}$. Then from Lemma 13, we have

$$\begin{aligned} & \left\| \left\| \mathbf{G}_k \mathbf{H}_k^\top \mathbf{Z}_k^a \mathbf{M}_0 \mathbf{Z}_k^a \mathbf{H}_k \mathbf{G}_k^\top \right\| \cdot 1(\mathcal{E}_k) \right\|_{\psi_1} \\ & \lesssim (\bar{r}_k \left\| \mathbf{H}_k^\top \mathbf{Z}_k^a \mathbf{M}_0 \mathbf{Z}_k^a \mathbf{H}_k \right\| + \text{tr}(\mathbf{H}_k^\top \mathbf{Z}_k^a \mathbf{M}_0 \mathbf{Z}_k^a \mathbf{H}_k)) \sigma_k^2 \\ & \leq (n \vee d_k) [C(nd_k + n^2)]^a \sigma_k^{4a+4} (\text{tr}(\mathbf{M}_0) + \bar{r}_k \|\mathbf{M}_0\|). \end{aligned} \quad (27)$$

Next we consider $\left\| \left\| \mathbf{H}_1^\top \mathbf{Z}_k^a \mathbf{M}_0 \mathbf{Z}_k^a \mathbf{H}_1^\top \right\| \cdot 1(\mathcal{E}_k) \right\|_{\psi_1}$. For simplicity, we denote $\mathbf{H}_2 \mathbf{H}_2^\top = \mathbf{H}_k \mathbf{H}_k^\top - \mathbf{H}_1 \mathbf{H}_1^\top$ and

$$\mathbf{Z}_k = \underbrace{\mathbf{H}_1 \mathbf{H}_1^\top}_{:=\mathbf{\Delta}_1} + \underbrace{\mathbf{H}_2 \mathbf{H}_2^\top - (d_k - \bar{r}_k) \mathbf{I}}_{:=\mathbf{\Delta}_2} + \underbrace{(-\bar{r}_k \mathbf{I})}_{:=\mathbf{\Delta}_3}.$$

Then we have

$$\begin{aligned} \text{tr}(\mathbf{H}_1^\top \mathbf{Z}_k^a \mathbf{M}_0 \mathbf{Z}_k^a \mathbf{H}_1^\top) \cdot 1(\mathcal{E}_k) &= \sum_{i_1, \dots, i_a, j_1, \dots, j_a \in [3]} \text{tr}(\mathbf{H}_1^\top \mathbf{\Delta}_{i_1} \cdots \mathbf{\Delta}_{i_a} \mathbf{M}_0 \mathbf{\Delta}_{j_1} \cdots \mathbf{\Delta}_{j_a} \mathbf{H}_1^\top) \\ &\leq 3^a \sum_{i_1, \dots, i_a \in [3]} \text{tr}(\mathbf{H}_1^\top \mathbf{\Delta}_{i_1} \cdots \mathbf{\Delta}_{i_a} \mathbf{M}_0 \mathbf{\Delta}_{i_a} \cdots \mathbf{\Delta}_{i_1} \mathbf{H}_1^\top). \end{aligned}$$

Then if one of i_1, \dots, i_a is equal to 3, then we have

$$\left\| \left\| \mathbf{H}_1^\top \mathbf{\Delta}_{i_1} \cdots \mathbf{\Delta}_{i_a} \mathbf{M}_0 \mathbf{\Delta}_{i_a} \cdots \mathbf{\Delta}_{i_1} \mathbf{H}_1^\top \right\| \cdot 1(\mathcal{E}_k) \right\| \leq n \bar{r}_k^2 [C(nd_k + n^2)]^{a-1} \sigma_k^{4a+2} \|\mathbf{M}_0\|.$$

Otherwise it takes the following form for some $0 \leq b \leq a$:

$$\begin{aligned} & \left\| \left\| \mathbf{H}_1^\top \mathbf{\Delta}_{i_1} \cdots \mathbf{H}_1 \mathbf{H}_1^\top \mathbf{\Delta}_2^b \mathbf{M}_0 \mathbf{\Delta}_2^b \mathbf{H}_1 \mathbf{H}_1^\top \cdots \mathbf{\Delta}_{i_1} \mathbf{H}_1^\top \right\| \cdot 1(\mathcal{E}_k) \right\|_{\psi_1} \\ & \leq n^2 \cdot [C(nd_k + n^2)]^{a-b-1} \sigma_k^{4a-4b} \left\| \left\| \mathbf{H}_1^\top \mathbf{\Delta}_2^b \mathbf{M}_0 \mathbf{\Delta}_2^b \mathbf{H}_1 \right\| \cdot 1(\mathcal{E}_k) \right\|_{\psi_1} \\ & \leq n^2 [C(nd_k + n^2)]^{a-b-1} [C(nd_k + n^2)]^b \sigma_k^{4a+2} (\text{tr}(\mathbf{M}_0) + \bar{r}_k \|\mathbf{M}_0\|) \\ & \leq \bar{r}_k [C(nd_k + n^2)]^a \sigma_k^{4a+2} (\text{tr}(\mathbf{M}_0) + \bar{r}_k \|\mathbf{M}_0\|), \end{aligned}$$

where in the second last inequality we use the fact \mathbf{H}_1 and $\mathbf{\Delta}_2$ are independent and the fact at the beginning of the proof. In conclusion we have (the term 3^a is absorbed into the absolute constant C)

$$\left\| \left\| \mathbf{H}_1^\top \mathbf{Z}_k^a \mathbf{M}_0 \mathbf{Z}_k^a \mathbf{H}_1^\top \right\| \cdot 1(\mathcal{E}_k) \right\|_{\psi_1} \leq [C(nd_k + n^2)]^a \sigma_k^{4a+2} (\text{tr}(\mathbf{M}_0) + \bar{r}_k \|\mathbf{M}_0\|).$$

Together with (27), we conclude

$$\left\| \text{tr}(\mathbf{Y}_k \mathbf{Z}_k^a \mathbf{M}_0 \mathbf{Z}_k^a \mathbf{Y}_k^\top) \cdot 1(\mathcal{E}_k) \right\|_{\psi_1} \leq [C(nd_k + n^2)]^a \sigma_k^{4a+2} (\text{tr}(\mathbf{M}_0) + \bar{r}_k \|\mathbf{M}_0\|) (1 + d_k \text{SNR}_k^{-2}).$$

D Technical Lemmas

Lemma 11. Let $\mathbf{V} \in \mathbb{R}^{n \times r_1}$, $\mathbf{W} \in \mathbb{R}^{d \times r_2}$. Assume \mathbf{V}, \mathbf{W} , $\begin{bmatrix} \mathbf{V} & \mathbf{W} \end{bmatrix}$ have full column rank, then we have that the operator norm of the (1, 2)-th block of

$$\begin{bmatrix} \mathbf{V}^\top \mathbf{V} & \mathbf{V}^\top \mathbf{W} \\ \mathbf{W}^\top \mathbf{V} & \mathbf{W}^\top \mathbf{W} \end{bmatrix}^{-r}$$

is bounded by $r\lambda^{-2r}\delta(1-\delta^2)^{-1}$, where λ is the smallest non-zero singular value of $\begin{bmatrix} \mathbf{V} & \mathbf{W} \end{bmatrix}$, and $\delta = \|(\mathbf{V}^\top \mathbf{V})^{-1/2} \mathbf{V}^\top \mathbf{W} (\mathbf{W}^\top \mathbf{W})^{-1/2}\|$.

Proof. Denote $\mathbf{\Gamma} = \begin{bmatrix} \mathbf{V}^\top \mathbf{V} & \mathbf{V}^\top \mathbf{W} \\ \mathbf{W}^\top \mathbf{V} & \mathbf{W}^\top \mathbf{W} \end{bmatrix}$, then we have $\|\mathbf{\Gamma}^{-1}\| \leq \lambda^{-2}$. As a result of Schur complement, we have the (1, 2)-th block of $\mathbf{\Gamma}^{-1}$ is equal to

$$-(\mathbf{V}^\top \mathbf{V})^{-1/2} \bar{\mathbf{V}}^\top \bar{\mathbf{W}} (\mathbf{I} - \bar{\mathbf{W}}^\top \bar{\mathbf{V}} \bar{\mathbf{V}}^\top \bar{\mathbf{W}})^{-1} (\mathbf{W}^\top \mathbf{W})^{-1/2},$$

where $\bar{\mathbf{V}} = \mathbf{V}(\mathbf{V}^\top \mathbf{V})^{-1/2}$, $\bar{\mathbf{W}} = \mathbf{W}(\mathbf{W}^\top \mathbf{W})^{-1/2}$. This implies $\|[\mathbf{\Gamma}^{-1}]_{12}\| \leq \lambda^{-2}\delta(1-\delta^2)^{-1}$.

Writing $\mathbf{\Gamma}^{-r} = \mathbf{\Gamma}^{-r+1} \cdot \mathbf{\Gamma}^{-1}$, and we have

$$\begin{aligned} \|[\mathbf{\Gamma}^{-r}]_{12}\| &\leq \|[\mathbf{\Gamma}^{-r+1}]_{11}\| \cdot \|[\mathbf{\Gamma}^{-1}]_{12}\| + \|[\mathbf{\Gamma}^{-r+1}]_{12}\| \cdot \|[\mathbf{\Gamma}^{-1}]_{22}\| \\ &\leq \lambda^{-2r+2} \cdot \lambda^{-2}\delta(1-\delta^2)^{-1} + \lambda^{-2r+2} \|[\mathbf{\Gamma}^{-r+1}]_{12}\|. \end{aligned}$$

Telescoping this inequality and we conclude $\|[\mathbf{\Gamma}^{-r}]_{12}\| \leq r\lambda^{-2r}\delta(1-\delta^2)^{-1}$. \square

Lemma 12. If we have for $A, B, C > 0$,

$$\mathbb{P}(|X| \geq A(t+C) + B\sqrt{t+C}) \leq 2\exp(-t),$$

for all $t > 0$, then we have

$$\|X\|_{\psi_1} \leq C_0 \left(AC + A + \frac{B^2}{A} \right).$$

for some absolute constant $C_0 > 0$.

Proof. Following the definition of ψ_1 norm, we compute $\mathbb{E} \exp(\frac{|X|}{K})$:

$$\mathbb{E} \exp\left(\frac{|X|}{K}\right) = \int_0^{+\infty} \mathbb{P}\left(\exp\left(\frac{|X|}{K}\right) \geq u\right) du = \int_{-\infty}^{+\infty} \mathbb{P}(|X| \geq x) \frac{1}{K} \exp\left(\frac{x}{K}\right) dx.$$

Notice

$$\int_{-\infty}^{2AC+2B\sqrt{C}} \mathbb{P}(|X| \geq x) \frac{1}{K} \exp\left(\frac{x}{K}\right) dx \leq \int_{-\infty}^{2AC+2B\sqrt{C}} \frac{1}{K} \exp\left(\frac{x}{K}\right) dx = \exp\left(\frac{2AC+2B\sqrt{C}}{K}\right).$$

Next we bound $\mathbb{P}(|X| \geq x)$ when $x \geq 2AC + 2B\sqrt{C}$. We set $x = A(t + C) + B\sqrt{t + C}$. Since $A(t + C) + B\sqrt{t + C}$ is a function increasing in t , we have $t \geq C$. Therefore

$$x = A(t + C) + B\sqrt{t + C} \leq 2At + 2B\sqrt{t} \leq \max\{4At, 4B\sqrt{t}\}.$$

This implies $t \geq \min\{\frac{x}{4A}, (\frac{x}{4B})^2\}$. And thus

$$\mathbb{P}(|X| \geq x) \leq 2 \exp(-t) \leq 2 \exp\left(-\min\left\{\frac{x}{4A}, \left(\frac{x}{4B}\right)^2\right\}\right) \leq \begin{cases} 2e^{-x^2/(4B)^2}, & x \leq \frac{4B^2}{A} \\ 2e^{-x/4A}, & x \geq \frac{4B^2}{A}. \end{cases}$$

Therefore

$$\begin{aligned} & \int_{2AC+2B\sqrt{C}}^{+\infty} \mathbb{P}(|X| \geq x) \frac{1}{K} \exp\left(\frac{x}{K}\right) dx \\ & \leq \int_{2AC+2B\sqrt{C}}^{\frac{4B^2}{A}} \mathbb{P}(|X| \geq x) \frac{1}{K} \exp\left(\frac{x}{K}\right) dx + \int_{\frac{4B^2}{A}}^{+\infty} \mathbb{P}(|X| \geq x) \frac{1}{K} \exp\left(\frac{x}{K}\right) dx \\ & \leq C_0 \frac{B}{K} \exp\left(\frac{B^2}{K^2}\right) + C_0 \exp\left(\frac{4B^2}{AK}\right) \end{aligned}$$

whenever $K \geq 8A$ and C_0 here is some absolute constant. In order to make $\mathbb{E} \exp(\frac{|X|}{K}) \leq 2$, we need to choose $K \geq C_0(AC + B\sqrt{C} + A + \frac{B^2}{A} + B)$. Notice $AC + \frac{B^2}{A} \geq 2B\sqrt{C}$ and $A + \frac{B^2}{A} \geq 2B$, it suffices to choose $K \geq C_0(AC + A + \frac{B^2}{A})$. \square

Lemma 13. Let $\mathbf{G} \in \mathbb{R}^{n \times r}$ be a random matrix whose entries \mathbf{G}_{ij} are independent mean-zero sub-gaussian random variables such that $\max_{ij} \|\mathbf{G}_{ij}\|_{\psi_2} \leq 1$. Then we have

$$\left\| \left\| \mathbf{G}^\top \mathbf{M}_0 \mathbf{G} \right\| \right\|_{\psi_1} \leq C_1 (\text{tr}(\mathbf{M}_0) + \|\mathbf{M}_0\|_r)$$

for SPSD matrix \mathbf{M}_0 and absolute constant $C_1 > 0$.

Proof. Using a standard ϵ -net argument, we have

$$\mathbb{P}\left(\left\|\mathbf{G}^\top \mathbf{M}_0 \mathbf{G} - \text{tr}(\mathbf{M}_0) \mathbf{I}_r\right\| \geq C_0 \|\mathbf{M}_0\| (t+r) + C_0 \|\mathbf{M}_0\|_F \sqrt{t+r}\right) \leq 2e^{-t}.$$

Then from Lemma 12, we have

$$\left\|\left\|\mathbf{G}^\top \mathbf{M}_0 \mathbf{G} - \text{tr}(\mathbf{M}_0) \mathbf{I}_r\right\|\right\|_{\psi_1} \leq C_0(\|\mathbf{M}_0\| + \frac{\|\mathbf{M}_0\|_F^2}{\|\mathbf{M}_0\|}).$$

And this leads to

$$\left\|\left\|\mathbf{G}^\top \mathbf{M}_0 \mathbf{G}\right\|\right\|_{\psi_1} \leq C_0\left(\|\mathbf{M}_0\| r + \frac{\|\mathbf{M}_0\|_F^2}{\|\mathbf{M}_0\|} + \text{tr}(\mathbf{M}_0)\right) \leq C_1(\text{tr}(\mathbf{M}_0) + \|\mathbf{M}_0\| r).$$

□

Lemma 14. *Let $\mathbf{X} \in \mathbb{R}^{m \times n}$ be a random matrix whose entries \mathbf{X}_{ij} are independent mean-zero sub-gaussian random variables. Then we have*

$$\left\|\left\|\mathbf{A}\right\|\right\|_{\psi_2} \leq c \cdot \max_{ij} \|\mathbf{X}_{ij}\|_{\psi_2} \sqrt{m+n}.$$

Proof. From (Vershynin, 2018, Theorem 4.4.5), we have

$$\mathbb{P}\left(\|\mathbf{X}\| \geq c \cdot \max_{ij} \|\mathbf{X}_{ij}\|_{\psi_2} (\sqrt{m+n} + t)\right) \leq 2e^{-t^2}.$$

Together with Lemma 15, we finalize the proof. □

Lemma 15. *If we have*

$$\mathbb{P}(|X| \geq C_0(K+t)) \leq 2 \exp(-t^2),$$

for all $t > 0$ and $K \geq 1$, then we have

$$\|X\|_{\psi_2} \leq 3C_0K.$$

Proof. We will show $\mathbb{P}(|X| \geq s) \leq 2 \exp(-s^2/(3C_0K)^2)$ for all $s > 0$. When $0 < s \leq 2C_0K$, we have

$$\mathbb{P}(|X| \geq s) \leq 1 \leq 2 \exp(-(2C_0K)^2/(3C_0K)^2) \leq 2 \exp(-s^2/(3C_0K)^2).$$

When $s > 2C_0K$, we have

$$\frac{s}{C_0} - K \geq \frac{s}{C_0} - \frac{s}{2C_0} = \frac{s}{2C_0}.$$

And thus $(\frac{s}{C_0} - K)^2 \geq \frac{s^2}{(2C_0)^2}$. So we conclude

$$\begin{aligned} \mathbb{P}(|X| \geq s) &= \mathbb{P}(|X| \geq C_0(K + \frac{s}{C_0} - K)) \\ &\leq 2 \exp(-(\frac{s}{C_0} - K)^2) \leq 2 \exp(-\frac{s^2}{(2C_0)^2}) \leq 2 \exp(-\frac{s^2}{(3C_0K)^2}), \end{aligned}$$

where in the last inequality we use $K \geq 1$. □